Discoveries

FORUM REVIEW ARTICLE

Simple Biological Systems for Assessing the Activity of Superoxide Dismutase Mimics

Artak Tovmasyan,[1] Julio S. Reboucas,[2] and Ludmil Benov[3]

Abstract

Significance: Half a century of research provided unambiguous proof that superoxide and species derived from it—reactive oxygen species (ROS)—play a central role in many diseases and degenerative processes. This stimulated the search for pharmaceutical agents that are capable of preventing oxidative damage, and methods of assessing their therapeutic potential. *Recent Advances:* The limitations of superoxide dismutase (SOD) as a therapeutic tool directed attention to small molecules, SOD mimics, that are capable of catalytically scavenging superoxide. Several groups of compounds, based on either metal complexes, including metalloporphyrins, metallocorroles, Mn(II) cyclic polyamines, and Mn(III) salen derivatives, or non-metal based compounds, such as fullerenes, nitrones, and nitroxides, have been developed and studied *in vitro* and *in vivo*. Very few entered clinical trials. *Critical Issues and Future Directions:* Development of SOD mimics requires in-depth understanding of their mechanisms of biological action. Elucidation of both molecular features, essential for efficient ROS-scavenging *in vivo*, and factors limiting the potential side effects requires biologically relevant and, at the same time, relatively simple testing systems. This review discuses the advantages and limitations of genetically engineered SOD-deficient unicellular organisms, *Escherichia coli* and *Saccharomyces cerevisiae* as tools for investigating the efficacy and mechanisms of biological actions of SOD mimics. These simple systems allow the scrutiny of the minimal requirements for a functional SOD mimic: the association of a high catalytic activity for superoxide dismutation, low toxicity, and an efficient cellular uptake/biodistribution. *Antioxid. Redox Signal.* 20, 2416–2436.

Introduction

Excessive production of reactive species derived from oxygen is implicated in various pathological processes. Promising results with superoxide dismutase (SOD) preparations (9,47,81) stimulated an intense search for pharmacological agents that combine highly efficient detoxification of superoxide radical ($O_2^{\bullet-}$) with minimal side effects. Advancement in understanding of the mechanisms of the SOD-catalyzed $O_2^{\bullet-}$ dismutation, and the fact that certain transition metal complexes are capable of substituting for the SODs, directed the efforts toward creation of functional, artificial SOD catalysts—SOD mimics. In a relatively short period, a variety of SOD mimics, often based on low-molecular-weight transition-metal complexes, were produced. Clinical trials, however, are limited mainly due to a lack of information about bioavailability, absorption, pharmacokinetics, toxicity, and biotransformation of such antioxidants. For many of them, it is not known whether they retain *in vivo* the activities assigned based on *in vitro* assays. The need to study *in vivo* the mechanisms of action of SOD mimics, and to predict which compounds might have potential medical applications, posed a strong demand for appropriate biological testing systems. Since all aerobic organisms inevitably generate superoxide, finding a suitable biosystem may appear easier than it actually is. Numerous articles report beneficial effects of SOD mimics in animal models of diseases and pathological conditions having oxidative stress as a common mechanism [for recent reviews, see (11,16,86,120)]. However, higher eukaryotic organism-based models are too complex, and biological activity of any studied agent depends on complicated pharmacokinetics, tissue gradient distribution, and others. In

[1]Department of Radiation Oncology, Duke University Medical Center, Durham, North Carolina.
[2]Departamento de Química, CCEN, Universidade Federal da Paraíba, João Pessoa, Brazil.
[3]Department of Biochemistry, Faculty of Medicine, Kuwait University, Kuwait City, Kuwait.

addition, the compound can be modified or degraded, obscuring the benefits that could arise from the superoxide dismuting ability of the potential SOD mimic itself. Since most SOD mimics display a variety of activities and do not selectively react with $O_2^{\bullet-}$, reported beneficial effects can be attributed to actions other than superoxide scavenging (54). Similar shortcomings apply to cell culture systems in which $O_2^{\bullet-}$, along with other reactive oxygen species (ROS), are generated by the addition of chemical agents (84,101), enzymatically (xanthine plus xanthine oxidase) (84), by radiation exposure (110); by activation of macrophages (33), and so on. The lack of a clear understanding of both the nature of the ROS responsible for damage and the mechanisms of action of the tested compounds can be listed among the reasons for failures in clinical trials (8,23,38,44,52,76,109). The use of so-called "SOD mimics" with low superoxide-scavenging activity casts doubt on mechanistic studies in which such compounds are applied "to prove" $O_2^{\bullet-}$ involvement.

At least some of the limitations of the more complicated systems listed earlier can be eliminated by simple, unicellular prokaryotic and eukaryotic organisms in which a high steady-state intracellular $O_2^{\bullet-}$ concentration can be maintained by aerobic metabolism, and where the effects of superoxide can be relatively easily quantified. The advantages of such microbial systems for studying the consequences of oxidative stress, elegantly summarized in a recent review (62), apply equally to the study of SOD mimics. Among such advantages are the selection of medium components to manipulate metabolic pathways, ability to grow under anaerobic as well as aerobic conditions, sufficient knowledge about pathways that are sensitive to $O_2^{\bullet-}$, and, most importantly, genetic manipulations producing mutants lacking specific ROS-scavenging enzymes.

Irrespective of their relative simplicity, even such unicellular organisms possess subcellular structures and metabolic activities that can noticeably modulate the bioefficacy and the mode of action of the tested SOD mimics. Similar to the multicellular eukaryotes, these simple organisms are well protected by SOD enzymes, which catalyze $O_2^{\bullet-}$ dismutation with a diffusion limited rate and, thus, overwhelm the action of any externally added SOD scavenger. This problem was solved by the use of mutants lacking SOD enzymes. The first such organism to be isolated was the unicellular eukaryote, *Saccharomyces cerevisiae* (34) followed by a prokaryote, *Escherichia coli* (35).

The SOD-Deficient Mutants

The SOD-deficient E. coli

The facultative anaerobe *E. coli* has three SOD isozymes. MnSOD and FeSOD are cytoplasmic and are encoded by the *sodA* and *sodB* genes, respectively (62,119). The third isozyme, a CuZnSOD, encoded by *sodC*, is periplasmic and is induced when bacteria enter a non-growing state, called stationary phase (25,32). In 1986, Carlioz and Touati (35) reported the construction of a *sodA sodB* mutant lacking the cytosolic MnSOD and FeSOD. The mutant is indistinguishable from its SOD-replete parent if grown in the absence of oxygen, but it aerobically exhibits defects directly resulting from the lack of cytoplasmic SODs. The defects include slow aerobic growth even in media containing all the required nutrients (1,35) and an inability to grow on non-fermentable carbon sources or in the absence of sulfur-containing (31), branched-chain (35), and aromatic (30) amino acids. Absence of cytoplasmic SODs was also associated with leaky membranes (64), sensitivity to mild heat shock (28), hypersensitivity to hydrogen peroxide (H_2O_2) and redox-cycling agents (35), and a high rate of spontaneous mutagenesis (29,49). All these defects can be eliminated by the expression of active SOD (87,118), which implies that a compound acting as an artificial SOD enzyme should have a similar effect. In addition, the auxotrophy (inability to synthesize a particular organic compound required for growth) for branched-chain, sulfur-containing, and aromatic amino acids can be suppressed by spontaneous mutations producing pseudorevertants that are capable of growing in aerobic minimal medium without expressing cytoplasmic SODs (63,64) or by supplementation of the growth medium with manganese salts (1).

The SOD-deficient S. cerevisiae

The unicellular eukaryote, *S. cerevisiae*, is commonly used as a single-cell model for higher eukaryotic organisms. As in the majority of eukaryotes, the most abundant SOD in *S. cerevisiae* is a cytoplasmic CuZnSOD (SOD1). It is also found in the nucleus and mitochondrial intermembrane space. In addition, eukaryotes express an MnSOD (SOD2) in the mitochondrial matrix. Similar to human MnSOD, and in contrast to bacterial MnSODs, which are dimers, *S. cerevisiae* MnSOD is a tetramer (94). Yeast with a mutated mitochondrial MnSOD gene (*sod2Δ*) are sensitive to oxygen (124). Under aerobic conditions, such mutants cannot grow on non-fermentable carbon sources, but do not show defects when grown on glucose. Strains with mutations in the cytoplasmic CuZnSOD gene (*sod1Δ*) are much more affected and show multiple defects. Similar to *sodA sodB E. coli*, they exhibit poor growth in normoxic conditions, increased mutation rate, decreased stationary phase survival (75), and amino-acid auxotrophies for lysine and methionine (34,60,129). Similarities with *sodA sodB E. coli* also include suppression of all growth defects by supplementation of the growth medium with manganese (106) or by growth under anaerobic conditions. The defects of *SOD1* mutants can be genetically reversed by mutations classified in two main groups. One group comprises mutations influencing transition metal ions homeostasis and includes the *BSD1* and *BSD2* (bypass SOD defects) genes (69). *BSD1* is identical to the *PMR1* gene, coding for a microsomal Ca^{2+} ATP-ase, which is eventually involved in the transport of other cations, including manganese. *BSD1* mutants accumulate elevated levels of intracellular manganese and copper (69), and it is known that Mn^{2+} can form unstable complexes that are capable of catalyzing $O_2^{\bullet-}$ dismutation (7,10). The *BSD2* gene codes for a protein that is important in copper ion transport and accumulation (74). Overexpression of another gene, *ATX1*, which is important in copper ion accumulation, also suppresses oxygen sensitivity of SOD-deficient yeast (70), which implies that Cu-containing complexes might play a protective role (77).

A second group consists of various mutations that suppress amino-acid auxotrophies without preventing hypersensitivity to oxidants (114).

The SOD-deficient E. coli *and* S. cerevisiae *as useful tools for screening of SOD mimics*

E. coli and *S. cerevisiae* strains containing deletions in the SOD genes could be considered very useful for the initial

screening of potential SOD mimics. As mentioned earlier, the lack of SODs in such organisms entails growth deficiencies, which can be relieved by active SOD or by a molecule that is capable of functionally substituting for it. Since SOD-deficient mutants aerobically grow slowly and cannot grow if certain amino acids are absent in the growth medium, most often, the activity of SOD mimics is assessed by their effect on the growth of the mutants. Growth is easy to follow turbidimetrically, and the rates of growth of the SOD-deficient mutants with and without the tested mimic are compared with those of the SOD-proficient parent.

This section describes growth media and general procedures for storage, inoculation, and growth of *E. coli* and *S. cerevisiae.*

Escherichia coli. *E. coli* frozen stocks are prepared by snap-freezing aliquoted overnight Luria–Bertani (LB) cultures (described below) preincubated for 30 min at room temperature with glycerol at a final concentration of 30%. In procedures used by different laboratories, frozen stock cultures are initially grown in LB medium. All media for *E. coli* growth are adapted from Sambrook *et al.* (105). LB medium contains 10 g of bactotryptone, 5 g of yeast extract, 10 g of sodium chloride (NaCl), and 2 g of glucose per liter. M9CA medium consists of M9 salts (components are listed next), 0.2% casamino acids, 0.2% glucose, 3 mg pantothenate, and 5 mg of thiamine per liter.

Among the restricted media, minimal medium is most often used. It consists of M9 salts supplemented with 3 mg of pantothenate, 5 mg of thiamine, and 2 g of glucose per liter. Filter-sterilized L-histidine, L-leucine, L-threonine, L-arginine, and L-proline (to 0.5 mM each) are added to satisfy the genetic auxotrophies of strains derived from AB1157. This medium is referred to as a five amino acid (5AA) medium. M9 salts are prepared by autoclaving 0.6 g of disodium phosphate, 0.3 g of monopotassium phosphate, 0.05 g of NaCl, and 0.1 g of ammonium chloride per liter in distilled water. After cooling, separately autoclaved solutions of magnesium sulfate and calcium chloride are added to a final concentration of 1.0 mM.

Liquid cultures. According to the simplest procedure, parental and SOD-deficient *E. coli* frozen stocks are initially inoculated in liquid LB medium, supplemented with appropriate antibiotics for the SOD-deficient mutants.

The LB culture is grown on a shaking water bath (200 rpm) under aerobic atmosphere for 24 h at 37°C. If compounds are to be tested in M9CA medium, the LB overnight culture is diluted into the medium usually to $A_{600nm} = 0.005$ ($\sim 5 \times 10^6$ cells/ml) [A_{600} of 1.0 = $\sim 1 \times 10^9$ cells/ml (85)]. If tests are carried out in a minimal/5AA medium, the cells are washed thrice with M9 salts to avoid transferring nutrients from LB to the minimal medium. The cells are then resuspended to A_{600} ~ 0.005 in 10–15 ml of minimal (or 5AA medium, depending on the genetic background of strains) and grown aerobically in 50 ml microbiological flasks.

As mentioned earlier, *sodA sodB* cultures tend to accumulate pseudorevertants that grow in aerobic minimal medium irrespective of the lack of cytoplasmic SODs (63). One way to suppress the growth of pseudorevertants is to grow the initial cultures under an anaerobic atmosphere (85% nitrogen, 10% hydrogen, and 5% carbon dioxide) in LB medium supple-

mented with 0.2% glucose (59). The overnight LB cultures are then diluted and grown overnight in anaerobic minimal medium. For testing SOD mimics, the anaerobic minimal cultures are diluted in minimal medium, and growth is followed under aerobic atmosphere.

Solid cultures. Another strategy for minimizing the overgrowth of suppressor mutants is to streak the frozen stocks on LB agar plates supplemented with 0.2% sucrose (64). In a procedure adopted by Munroe and coworkers (85), the agar plates are incubated in air for 24 h at 37°C. To ensure that the response is not specific for a particular clone, four independent colonies for each strain are each inoculated into 3.0 ml LB sucrose and grown overnight in air at 37°C and 220 rpm. The overnight 3.0 ml cultures are then inoculated in 15 ml LB-sucrose to $A_{600} = 0.01$ (parental) or 30 ml LB-sucrose to $A_{600} = 0.02$ (*sodA sodB*) in 50 ml culture flasks. After incubation for 2–3 h at 37°C and 220 rpm, the cells are washed thrice with minimal medium and resuspended in the same medium to the initial volume. Experimental cultures are prepared by diluting the cell suspension 1/10 with minimal or 5AA medium.

Growth is usually monitored turbidimetrically at 600 nm or if metalloporphyrins are tested, at 700 nm, in order to minimize the contribution of the absorbance of the compounds (50).

Until recently, test cultures were standardly grown in 50 ml flasks on a shaker at 200 rpm and 37°C, which limited the number of compounds that could be tested simultaneously. The use of 96-well microtiter plates, instead, has allowed simultaneous comparisons of a large number of compounds at a wide range of concentrations, but requiring minimal amounts of the tested compounds (85). The microtiter plates (100 μl of cell suspension per well) are usually shaken at 220 rpm in a 37°C incubator. Growth is measured by recording turbidity at 600 nm using a microtiter plate reader.

Saccharomyces cerevisiae. Using CuZnSOD-deficient *S. cerevisiae* as a biosensor for antioxidants was first proposed by Zyracka *et al.* (131). Three possible tests were listed, based on the estimation of lifespan, abolition of superoxide-induced auxotrophy, and growth in hypertonic medium. As with *E. coli*, a turbidimetric growth-based assay appears to be the easiest and the most often applied.

Two types of media are used for initial growth and for testing compounds: (i) YPD, a standard complete medium, contains 1% yeast extract and 2% peptone. Glucose (dextrose) is separately autoclaved and added to a final concentration of 2%. (ii) Synthetic (defined) dextrose medium (SD) is made of 1.8 g yeast nitrogen base (without amino acids and ammonium sulfate), 5.0 g ammonium sulfate, and 0.7 g monosodium phosphate. The pH is adjusted to 6.0 with 10 M sodium hydroxide. The SD medium is supplemented with glucose to 2%, and appropriate amino acids (SDC medium) (125).

For a routine pregrowth, the strains lacking CuZnSOD activity are cultured in microaerophilic conditions (5% oxygen) using CampyPaks (BBL) for plates or, for liquid cultures, 5 ml of medium in a 16 × 100 mm culture tube. For flask cultures, the low aeration is achieved by decreasing the surface-to-volume ratio and/or reducing the shaking rate to 100 rpm. High aeration for experimental samples is achieved by using a flask volume/medium volume ratio of 5:1 (typically 50 ml of medium in a 250-ml flask) and shaking at 200 rpm (41).

In the procedure described by Munroe *et al.* (85), 20% glycerol freezer stocks were streaked onto YPD agar plates and were grown under low oxygen at 30°C for 3 days. Precultures were prepared by inoculating single colonies in 5 ml of SD medium in 16 ml culture tubes and growing them overnight at 30°C and 220 rpm. Experimental cultures were then inoculated at $A_{600} = 0.05$ ($\sim 5 \times 10^5$ cells/ml; $A_{600} = 1.0$ corresponds to $\sim 1 \times 10^7$ cells/ml) in 10 ml liquid medium in 50 ml flasks and grown in air at 30°C and 220 rpm. Usually two to four independent colonies are used for each experiment.

In general, slight variations in the procedures used by different laboratories practically do not affect experimental outcomes, and if all precautions to avoid artifacts are taken into consideration, reported results about the efficacy of the tested redox-active compounds are consistent.

The Physico-Chemical Properties and the Biological Effects of SOD Mimics

The requirements for a good SOD mimic

A list of requirements for a compound to mimic SOD *in vivo* can be found in a publication by Czapski and Goldstein (40). Theoretically, an SOD mimic should exert protective effects by scavenging $O_2^{\bullet -}$ before it reacts with [4Fe-4S] clusters (71) or with other cellular targets (55). The efficiency of this process would depend on the concentration of the SOD mimic, its specificity (39), and the rate constant for reaction with $O_2^{\bullet -}$. Keeping in mind that the SOD mimic should outcompete biological superoxide targets and should complement endogenous SOD enzymes, it becomes clear that the SOD mimic should react with $O_2^{\bullet -}$ with a rate constant comparable to that of the SOD enzymes and should be present at comparable concentrations. This is not easily achievable, because SOD-catalyzed dismutation occurs at a rate of $> 10^9\ M^{-1}\ s^{-1}$ (56) and intracellular SODs reach a concentration of 10–20 μM (62).
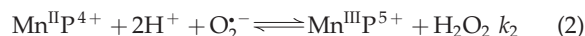
Alternatively, if catalytic activity is lower, the SOD mimic should accumulate at proportionally higher concentrations at the site of action. This, in turn, implies that in addition to catalytic activity, information about uptake and subcellular distribution of SOD mimics is essential for proper evaluation of their action. Caution should be exercised in interpreting data when compounds with low reactivity toward $O_2^{\bullet -}$ exert noticeable protection. Unless the tested compound preferentially accumulates at the sites of $O_2^{\bullet -}$ production, its effects are most probably due to actions other than $O_2^{\bullet -}$ scavenging.

Most of our current knowledge about the mechanisms of action and potential pitfalls in applying SOD mimics *in vivo* has been obtained using unicellular SOD-deficient organisms as a model system.

The mechanism of action of Mn porphyrins in SOD-deficient E. coli: preliminary insights

Faulkner *et al.* (50) were the first to use *sodA sodB E. coli* for determining the biological activity of several Mn porphyrins (MnPs), including MnTM-4-PyP^{5+} and MnTBAP^{3-} [Mn(III) *meso*-tetrakis(4-benzoic acid) porphyrin, also known as MnTCPP^{3-} and AEOL10201)] (Figs. 1 and 3). These researchers made the important observation that intracellular MnTM-4-PyP^{5+} looks greenish, suggesting that it exists in its reduced form, as Mn(II)TM-4-PyP^{4+} (50). This observation

helped explain the *in vivo* mechanism of catalytic $O_2^{\bullet -}$ removal by MnP-based SOD mimics. Reduction of MnTM-4-PyP^{5+} by cellular reductants (some reaching millimolar intracellular concentrations) rather than by $O_2^{\bullet -}$, avoids the rate-limiting first step of MnP-catalyzed $O_2^{\bullet -}$ dismutation [equation (1)]. Under such conditions, an MnP would act as superoxide reductase rather than SOD (50).

$$Mn^{III}P^{5+} + O_2^{\bullet -} \rightleftharpoons Mn^{II}P^{4+} + O_2\ k_1 \qquad (1)$$

$$Mn^{II}P^{4+} + 2H^+ + O_2^{\bullet -} \rightleftharpoons Mn^{III}P^{5+} + H_2O_2\ k_2 \qquad (2)$$

The importance of the growth medium

Since SOD deficiency slows the multiplication of microorganisms even in media containing all needed nutrients (35), the simplest way to test a potential SOD mimic would be to determine whether it restores the growth rate of the mutants to that of the SOD-replete parents. Evaluating potential SOD mimic in complete medium, however, poses a risk of erroneously taking for an SOD mimic a compound that stimulates the growth by an action other than catalytic scavenging of $O_2^{\bullet -}$. In complete (M9CA) medium, MnTBAP^{3-} accelerated the aerobic growth of the *sodA sodB E. coli* (50). MnTBAP^{3-}, however, has neither the thermodynamic nor kinetic properties needed to act as an SOD mimic (98) and does not help the aerobic growth of SOD-deficient *E. coli* in medium lacking aromatic, sulfur-containing, and branched-chain amino acids, such as 5AA medium (Fig. 2) (13). The lack of superoxide scavenging activity of MnTBAP^{3-} has been confirmed when tested on *sod1Δ S. cerevisiae* (85). These results point to the importance of using restricted medium for growth of *sodA sodB E. coli* when evaluating the potential of an SOD mimic.

Ortho, meta, and para Mn(III) N-alkylpyridylporphyrins

The importance of appropriate growth medium for assessing SOD mimics was further supported when the effects of *ortho*, *meta*, and *para* isomers of MnTMPyP^{5+} [MnTM-2(or 3, or 4)-PyP^{5+}] were compared in cultures grown in different media (12) (Figs. 3 and 4). In M9CA medium, all three isomers stimulated the aerobic growth of the *sodA sodB* strain. Growth in 5AA medium, however, revealed clear differences among the isomers; the *ortho* isomer was the most efficient in stimulating the growth of the SOD-deficient mutant, the *meta* isomer was similar, while the *para* isomer did not show any beneficial effect (Fig. 4) (12). Among the reasons for the lack of beneficial effect of the *para* isomer *in vivo* is the intercalation of its more planar molecule (relative to the *ortho* and *meta* isomers) in DNA, leading to toxicity and loss of SOD activity (50).

Does catalytic activity predict the biological activity?

Since high catalytic activity [$k_{cat}(O_2^{\bullet -})$] of a potential SOD mimic is considered the main factor contributing to its biological efficacy, efforts were directed toward bringing the $k_{cat}(O_2^{\bullet -})$ values of MnPs closer to the $k_{cat}(O_2^{\bullet -})$ values of the SOD enzymes. Testing the effect of such compounds on *sodA sodB E. coli*, however, revealed that a high $k_{cat}(O_2^{\bullet -})$ does not necessarily translate into a high biological efficacy. To
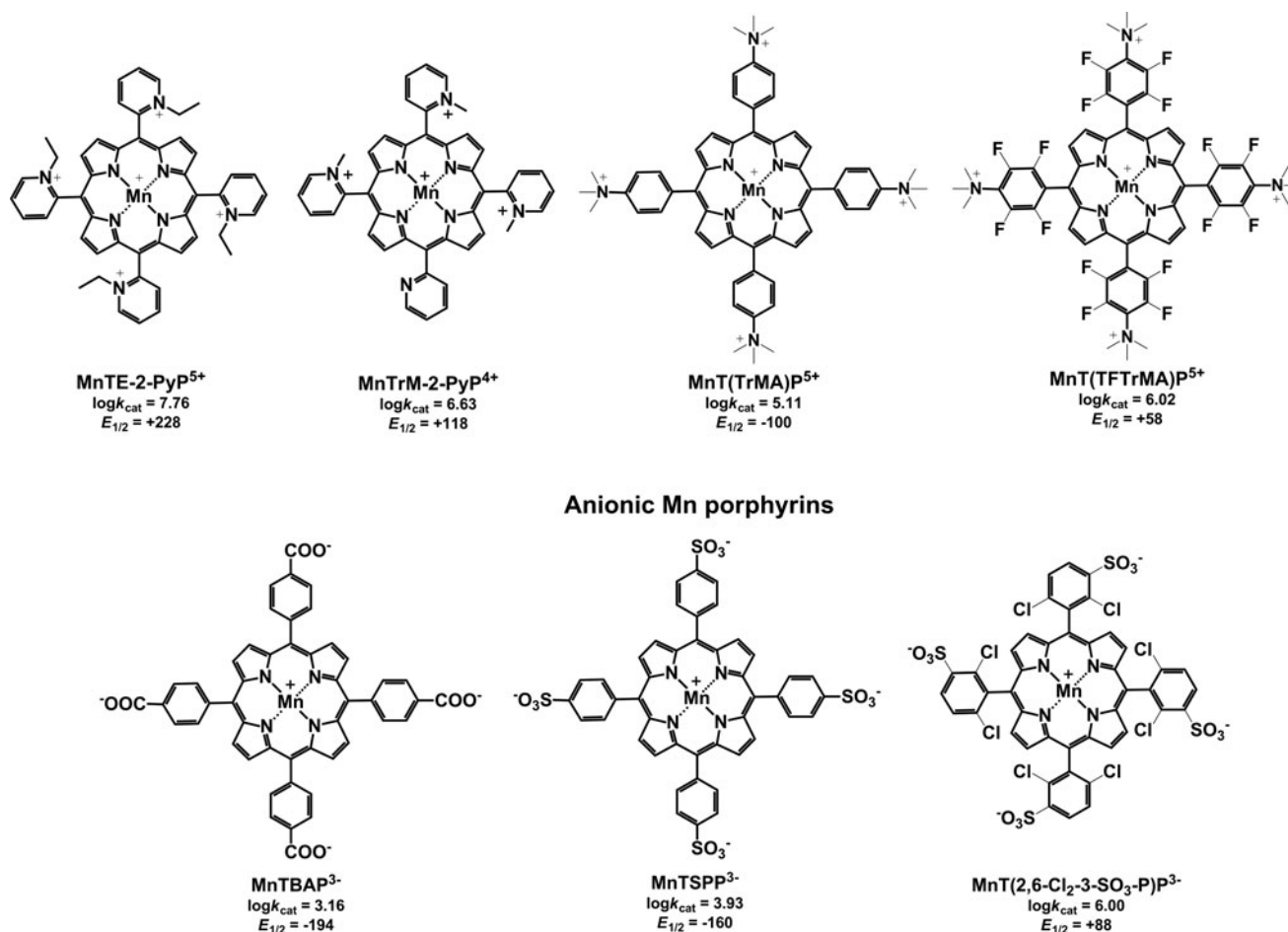
MnTE-2-PyP^{5+}
log k_{cat} = 7.76
$E_{1/2}$ = +228

MnTrM-2-PyP^{4+}
log k_{cat} = 6.63
$E_{1/2}$ = +118

MnT(TrMA)P^{5+}
log k_{cat} = 5.11
$E_{1/2}$ = -100

MnT(TFTrMA)P^{5+}
log k_{cat} = 6.02
$E_{1/2}$ = +58

Anionic Mn porphyrins

MnTBAP^{3-}
log k_{cat} = 3.16
$E_{1/2}$ = -194

MnTSPP^{3-}
log k_{cat} = 3.93
$E_{1/2}$ = -160

MnT(2,6-Cl$_2$-3-SO$_3$-P)P^{3-}
log k_{cat} = 6.00
$E_{1/2}$ = +88

FIG. 1. **Chemical structures, superoxide dismutase activity (catalytic rate constant for $O_2^{\bullet-}$ dismutation, log k_{cat}), and Mn^{III}/Mn^{II} reduction potential ($E_{1/2}$ in mV *vs.* normal hydrogen electrode) of various cationic and anionic Mn porphyrins.**

increase the catalytic activity of MnP-based SOD mimics, the pyrrolic moiety was derivatized with electron-withdrawing groups (*e.g.*, Br and Cl), which stabilized Mn in the +2 oxidation state, instead of the +3 state usually found in the non-derivatized analogs. The electron-deficient ligand produced by such modification cannot support the higher Mn +3 oxidation state. Thus, no oxidation occurs on metallation of the ligand with manganese(II) chloride (MnCl$_2$), and Mn complex bearing Mn in the +2 oxidation state was isolated. With β-octabrominated MnBr$_8$TM-4-PyP^{4+} [log $k_{cat} \geq 8.67$, $E_{1/2} = +480$ mV *vs.* normal hydrogen electrode (NHE)] (14) and MnBr$_8$TM-3-PyP^{4+} (log $k_{cat} \geq 8.85$, $E_{1/2} = +468$ mV *vs.* NHE) (42), catalytic activity and reduction potentials comparable to those of the SOD enzymes (log $k_{cat} = 8.84$–9.30, $E_{1/2} + 300$ mV *vs.* NHE) were achieved (42). When tested on *sodA sodB E. coli*, however, MnBr$_8$TM-3-PyP^{4+} demonstrated a concentration-dependent protection with maximum growth rate (~50% of that of the parent) reached at 1.0 μM (Fig. 5) (42). Higher concentrations were toxic. The *para* isomer was toxic even at 1 μM, and the maximum effect achieved at 0.5 μM was only ~30% growth compared with the parental strain (Fig. 5). The reason for such low efficacy *in vivo* can be found in the very low stability constant (*K*) of these perbrominated MnPs (log *K* = 8 for MnBr$_8$TM-4-PyP^{4+}). Consequently, they rapidly decompose, presumably generating toxic products. These results highlight the fact that

the high catalytic activity for $O_2^{\bullet-}$ dismutation is not a sufficient predictor of biological efficacy. Stability of the compound, its cellular uptake, subcellular distribution, and biological transformations are factors that could override the impact of k_{cat}.

The accumulation of MnPs by E. coli *and* S. cerevisiae

In general, the main features that determine the uptake and subcellular distribution of an externally added compound are (i) charge, (ii) shape and size, and (iii) lipophilicity of the molecule.

Charge. Comparison between anionic [MnT(2,6-Cl$_2$-3-SO$_3$-P)P^{3-}, MnTSPP^{3-}, and MnTBAP^{3-}] and cationic [MnTrM-2-PyP^{4+}, MnTE-2-PyP^{5+}, MnT(TFTrMA)P^{5+}, and MnT(TrMA)P^{5+}] MnPs (Fig. 1) revealed that positive charge is essential for biological activity (19). Cellular/mitochondrial uptake of positively charged molecules is driven by the membrane potential, which thermodynamically favors their accumulation to levels exceeding those of the surrounding medium. The importance of positive charges is illustrated by the fact that none of the anionic compounds could substitute for the missing cytoplasmic SODs in *E. coli*. Among the cationic MnPs tested, MnTM-2-PyP^{5+} (Fig. 3) and MnTE-2-PyP^{5+} (Fig. 1), with an $E_{1/2}$ close to the potential of the SOD
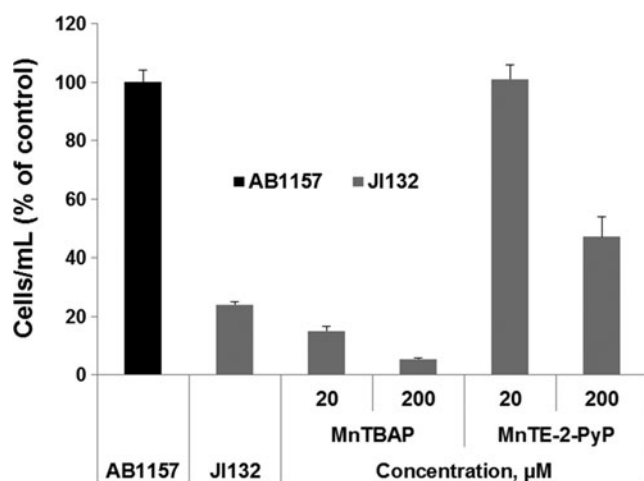
FIG. 2. **Cell density (based on A_{600}) of SOD-deficient *Escherichia coli* (JI132) after 20 h of growth.** Cultures were grown in the presence of 20 or 200 μM MnTE-2-PyP^{5+} and MnTBAP^{3-} in five amino acid medium. The A_{600} of parental (SOD-proficient, AB1157) *E. coli* strain was set at 100%. Adapted from (13). SOD, superoxide dismutase.

FIG. 4. **Aerobic growth of SOD-deficient *E. coli* (JI132) in five amino acid medium in the absence or presence of 25 μM *ortho* MnTM-2-PyP^{5+}, *meta* MnTM-3-PyP^{5+}, and *para* MnTM-4-PyP^{5+} isomers.** Growth was monitored turbidimetrically at 700 nm. The parental strain AB1157 was used as a control. Adapted from (12).

enzyme of +300 mV, accelerate the aerobic growth of the *sodA sodB* mutant to a rate typical for the SOD-containing parent (Fig. 6). These two cationic MnPs with a log $k_{cat}(O_2^{\bullet-}) \sim 7.8$ remain the most active and the least toxic, and are among the most studied MnPs in animal models of oxidative stress (21,22,43,108). They are commonly used as a positive control in SOD-deficient *E. coli* and *S. cerevisiae* studies. Anionic MnPs of low metal-centered reduction potentials (insufficiently redox-active) such as MnTBAP^{3-} (log $k_{cat} = 3.16$ and $E_{1/2} = -194$ mV *vs.* NHE), which repel the anionic $O_2^{\bullet-}$, cannot act as SOD mimics and do not protect the SOD-deficient *E. coli* (Fig. 2). Therefore, the therapeutic efficacy of MnTBAP^{3-} is likely based on a mechanism other than $O_2^{\bullet-}$ scavenging (13).

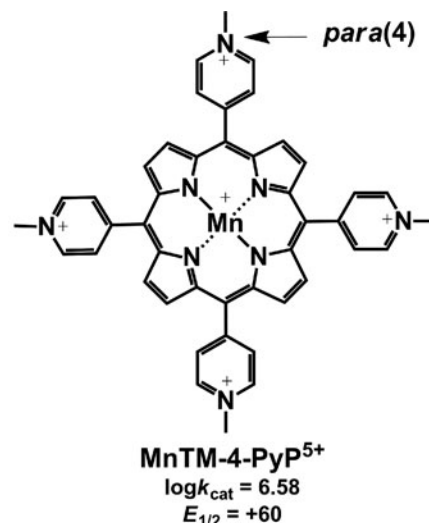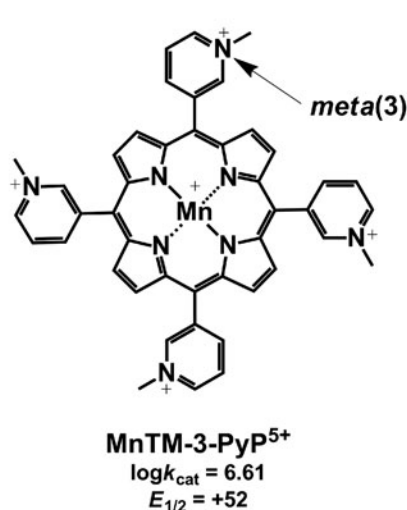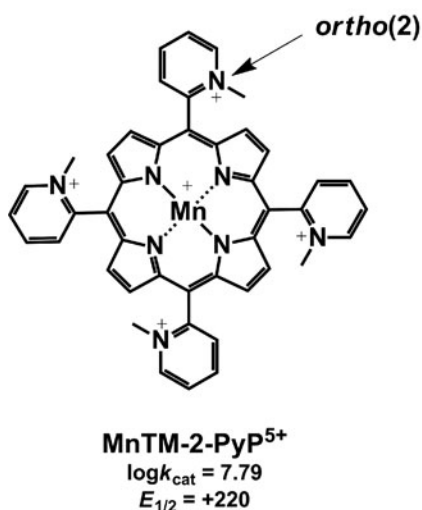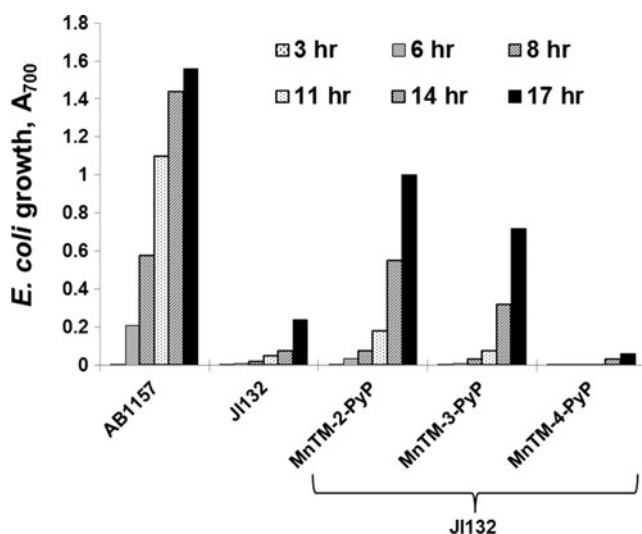**Shape and size of the molecule.** The three-dimensional structure of the molecule exerts a strong influence on the

biological efficacy of the SOD mimics. For example, the $k_{cat}(O_2^{\bullet-})$ of the *meta* isomers (alkyl side chain varying from methyl to octyl) is an order of magnitude lower than $k_{cat}(O_2^{\bullet-})$ of the corresponding *ortho* isomers, and their redox potentials differ significantly. $E_{1/2}$ of the *meta* MnP compounds falls in the region of 52–74 mV *versus* NHE, while for the *ortho* analogs, it is in the range from 220 to 367 mV *versus* NHE, depending on the nature of the alkyl side chains (11,122). Nevertheless, both *ortho* and *meta* analogs efficiently substituted for SOD when tested on *sodA sodB E. coli* (Fig. 6). In contrast, Mn(III) *N,N'*-disubstituted imidazolium analogs (MnTDE-2-ImP^{5+}, MnTM,MOE-2-ImP^{5+}, and MnTDMOE-2-ImP^{5+}, Fig. 7) despite having lipophilicity (R_f) comparable to and a k_{cat} similar to or even higher than that of their

FIG. 3. **Chemical structure, Mn^{III}/Mn^{II} reduction potential ($E_{1/2}$ in mV *vs.* normal hydrogen electrode), and SOD activity (catalytic rate constant for $O_2^{\bullet-}$ dismutation, log k_{cat}) of *ortho*, *meta*, and *para* isomers of MnTMPyP^{5+}.**
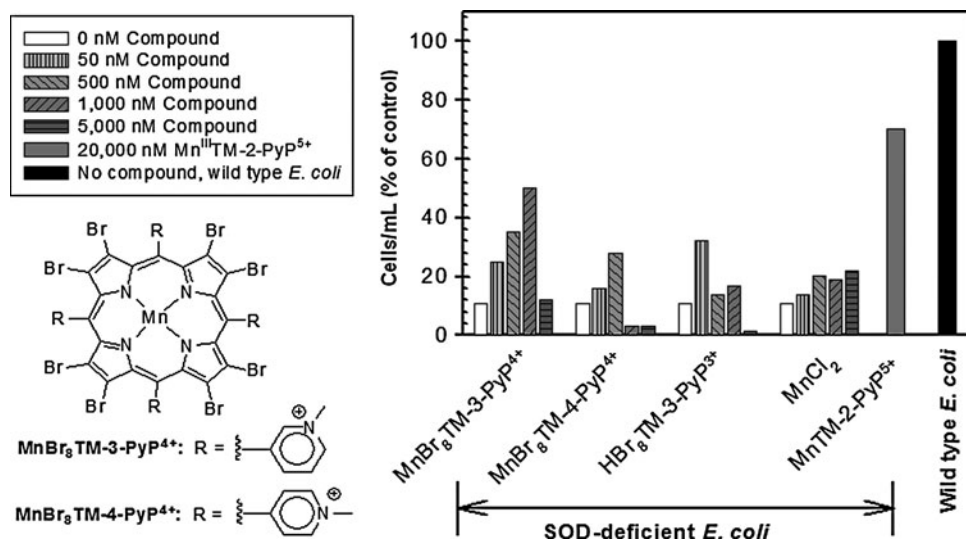
FIG. 5. Effect of β-brominated Mn(II) N-alkylpyridylporphyrins and their metal-free ligands on the growth of SOD-deficient E. coli in five amino acid medium. Cell density at the 13th hour of growth is presented. Adapted from (42).

N-substituted pyridyl analogs, MnTM-2-PyP^{5+} and MnTE-2-PyP^{5+}, were biologically much less efficient (Fig. 8). Such low bioefficacy could be attributed to the bulkiness of the molecule due to the N,N'-imidazolyl substituents located above and below the porphyrin plane (19), which hinders the diffusion across the membranes and prevents a sufficient cellular uptake.

Lipophilicity. Investigations of the relationship between MnP lipophilicity, influenced by the length of the aliphatic chains attached to the *meso* pyridyl nitrogen atoms at the porphyrin ring, and biological activity, have demonstrated that more lipophilic SOD mimics (MnTnHex-2-PyP^{5+} and MnTnOct-2-PyP^{5+}) are efficacious at lower concentrations

(0.1–3.0 μM); whereas less lipophilic compounds, MnTM-2-PyP^{5+}, MnTE-2-PyP^{5+}, and MnTnPr-2-PyP^{5+}, are highly efficient only at concentrations above 10 μM (Fig. 9) (88). Since all tested SOD mimics have similar log $k_{cat}(O_2^{\bullet-})$ values, the higher biological activity of the more lipophilic compounds could be attributed to more efficient cellular uptake resulting from facilitated diffusion across membranes.

Figure 10A shows that those MnPs which have high catalytic rate constants for $O_2^{\bullet-}$ dismutation ($>10^7 M^{-1} \cdot s^{-1}$) and protect the SOD-deficient mutants against $O_2^{\bullet-}$, accumulate in cells to concentrations that are comparable to or exceed those of the native SOD. The figure also shows that cellular accumulation of the most lipophilic Mn-hexyl derivatives is ~20–30-fold higher than the accumulation of the hydrophilic Mn-methyl derivatives, which explains why amphiphilic MnPs are efficient at concentrations lower than 1.0 μM.

These findings helped formulate the key requirements that should be met by the compounds expected to act as SOD mimics *in vivo*: high $k_{cat}(O_2^{\bullet-})$, high stability, and efficient cellular uptake.

Investigations of the relationship between MnPs lipophilicity and their cellular uptake and distribution, carried out with E. coli and S. cerevisiae, revealed the general rules that are applicable to higher organisms: (i) Longer aliphatic chain analogs with lipophilic properties accumulate in cytosol and membranes to higher levels than more hydrophilic molecules. *Meta* isomers, which are more flexible and more lipophilic (Fig. 10B), cross cell membranes easier than their respective *ortho* analogs, and are found in the cytosol at higher concentrations (Fig. 10A); and (ii) *in vivo*, a lower k_{cat} for $O_2^{\bullet-}$ dismutation can be compensated for by better cellular uptake of the SOD mimic, resulting in higher efficacy (Fig. 6) (66). Compensation for low catalytic activity by higher uptake, however, is limited by potential toxicity of the SOD mimics.

Cellular uptake of MnPs could be significantly influenced by the components of the growth medium. Reducing compounds, such as ascorbate, could significantly enhance the uptake of MnPs (Fig. 10C) (111). Reduction of Mn^{III}P to Mn^{II}P by ascorbate leads to the loss of a single charge at the metal center, which decreases the overall charge of the molecule from +5 to +4 and increases the lipophilicity of the
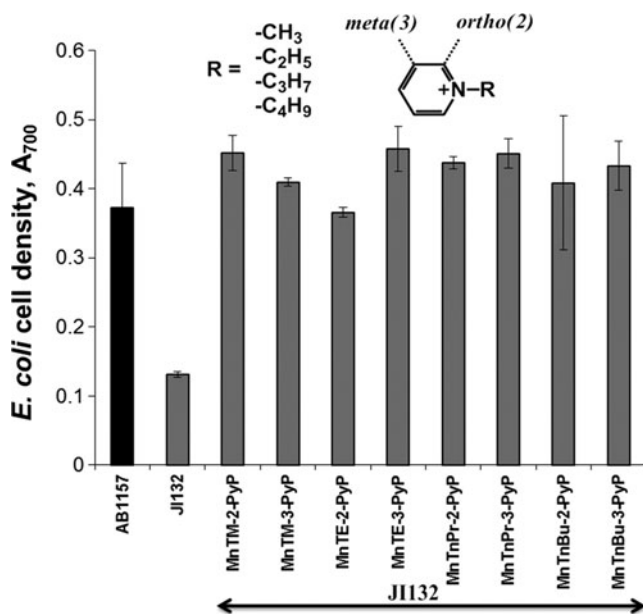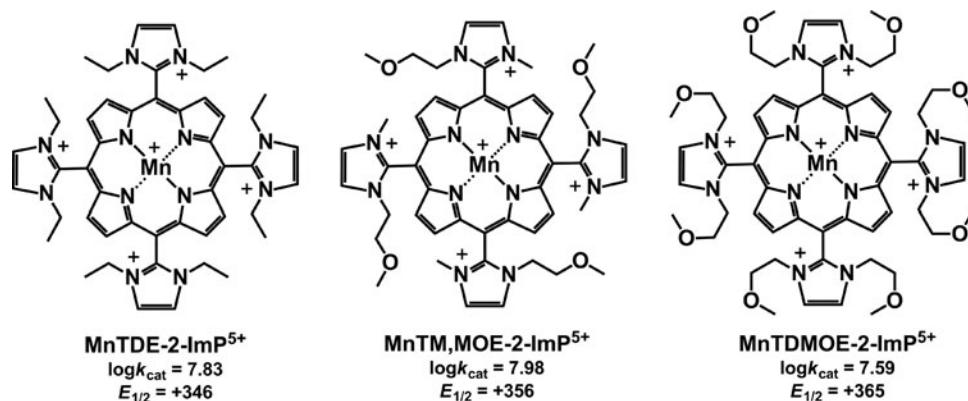

FIG. 6. Effect of 25 μM *ortho* (2) and *meta* (3) isomeric Mn(III) N-alkylpyridyl porphyrins (alkyls being methyl to butyl) on the aerobic growth of SOD-deficient E. coli (JI132) in five amino acid medium. Growth was monitored turbidimetrically at 700 nm. Cell density at 18 h is presented. Adapted from ref. (66).

FIG. 7. Structures, Mn^{III}/Mn^{II} reduction potential ($E_{1/2}$ in mV *vs.* normal hydrogen electrode), and SOD-like activity (catalytic rate constant for $O_2^{\bullet-}$ dismutation, log k_{cat}) of Mn(III) *N,N'*-disubstituted imidazolium porphyrins: MnTDE-2-ImP^{5+}, MnTM,MOE-2-ImP^{5+}, and MnTDMOE-2-ImP^{5+}. The imidazolium compounds have two imidazolyl substituents, one placed below and the other placed above the porphyrin ring, which makes them bulkier than *N*-substituted pyridylporphyrins (19).

metalloporphyrin. The importance of the metal center reduction is illustrated by the fact that the uptake of *meta* isomeric MnP, MnTM-3-PyP^{5+} was not affected by ascorbate. MnTM-3-PyP^{5+}, with a reduction potential of only 52 mV is much less reducible than the *ortho* analog, MnTM-2-PyP^{5+} with $E_{1/2}$ +220 mV *versus* NHE. While the *ortho* isomer exists as Mn^{II}TM-2-PyP^{4+} in biological milieu, the *meta* isomer remains unchanged, as a pentacationic species. Based on such observations, one could predict that in higher organisms, cellular/subcellular accumulation and distribution of SOD mimics may be strongly affected by endogenous reductants, some of which reach millimolar intracellular levels.

Studies on the subcellular localization of SOD mimics revealed similarities among different classes of organisms. A positive correlation between the lipophilicity and accumulation in mitochondria relative to the cytosol was observed in yeast cells incubated with a series of MnP analogs. For the least lipophilic compound, MnTM-2-PyP^{5+}, the mitochondria to cytosol ratio was ~1.5; while for the much more lipophilic MnTnHex-2-PyP^{5+}, the ratio was >10, that is, the concentration was 10-fold higher in the mitochondria than in the cytosol. Compounds of intermediate lipophilicity, MnTE-2-PyP^{5+} and MnTnBu-2-PyP^{5+}, showed intermediate distribu-

tion, with ratios of around 2 and 4, respectively (Li *et al.*, unpublished observation) (112). A similar distribution was found when MnPs were administered to mice. The mitochondria-to-cytosol ratio was 3.6 for MnTnHex-2-PyP^{5+} and 1.6 for MnTE-2-PyP^{5+} (126). The reason for such similarities lies in the identical forces and principles that govern cellular transport. Uptake of cationic metalloporphyrins by *E. coli* and mitochondria of eukaryotic cells is driven by the electrochemical proton gradient across membranes and is facilitated by the amphiphilic properties of the molecule. Depending on the alkyl chain length, MnPs accumulate more in membranes or in cytosol; the longer alkyl-chain analogs tend to accumulate more in membranes than in cytosol (66).

The toxicity of porphyrins

Toxicity is the main factor restricting the use of metalloporphyrin-based SOD mimics. Studies with various classes of organisms have shown that bacteria are much more sensitive to the toxicity of metalloporphyrins than other organisms, including the yeast *S. cerevisiae*.

Light-independent porphyrin toxicity to bacteria is well known, and has been proposed as a treatment modality against antibiotic-resistant strains (113). Several possible mechanisms of porphyrin toxicity have been suggested: interference with redox reactions, generation of ROS, distortion of the membrane lipid bilayer, and insertion of a nonfunctional heme-like porphyrin in heme-containing proteins, thus blocking their functions (113).

E. coli responds to oxidative stress by inducing specific regulons, which, in turn, prompt the expression of hundreds of genes [reviewed in details in (37,62)]. Activation of this response can serve as an indication of toxicity due to the reversed action of the tested SOD mimics, that is, pro-oxidative instead of antioxidative. For example, increased production of ROS explains the toxicity of some MnPs when they are combined with natural reductants. Such MnPs can be easily reduced by ascorbate, tetrahydrobiopterin, or glutathione (18,21,130) and can be subsequently reoxidized by either $O_2^{\bullet-}$ or dioxygen, generating H_2O_2 as an ultimate product. Reductants, usually present in all cells, can sustain the redox cycling, generating toxic levels of H_2O_2 (Fig. 11A) (15). *E. coli*
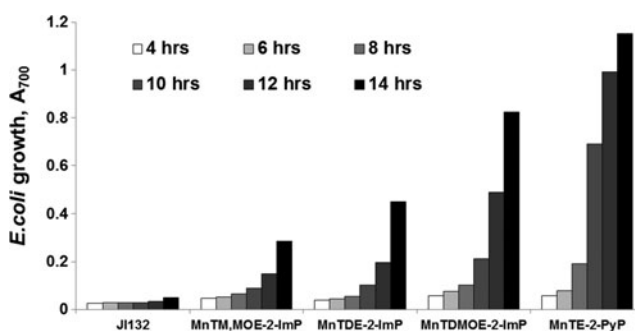

FIG. 8. Growth of SOD-deficient *E. coli* in five-amino-acid medium in the presence of 25 μM Mn(III) *N,N'*-disubstituted imidazolium porphyrins: MnTDE-2-ImP^{5+}, MnTM,MOE-2-ImP^{5+}, and MnTDMOE-2-ImP^{5+}. Their *N*-substituted pyridyl analog, MnTE-2-PyP^{5+}, was also tested for comparison. Adapted from (88).
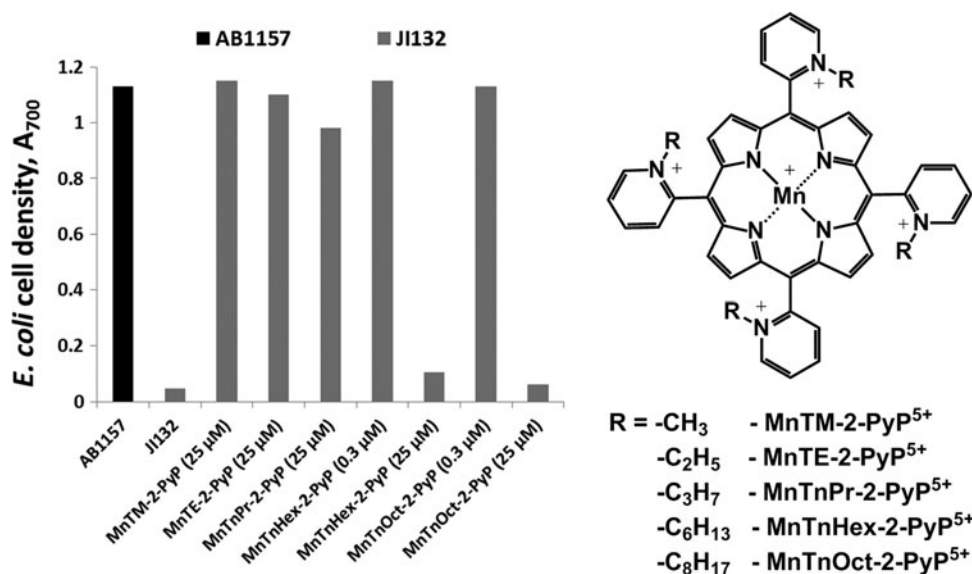
FIG. 9. Aerobic growth of SOD-deficient *E. coli* (JI132) in the presence of 25 μM Mn(III) *meso*-tetrakis(*N*-alkylpyridinium-2-yl)porphyrins, where the alkyl group is methyl (MnTM-2-PyP[5+]), ethyl (MnTE-2-PyP[5+]), n-propyl (MnTnPr-2-PyP[5+]), n-hexyl (MnTnHex-2-PyP[5+]), or n-octyl (MnTnOct-2-PyP[5+]) in restricted (5AA) medium. Data from 14 h of growth are shown. MnTnHex-2-PyP[5+] and MnTnOct-2-PyP[5+] were toxic at a 25 μM concentration but supported the growth of *E. coli* when supplied at a concentration as low as 0.3 μM. Adapted from (88).

reacts to the combination of MnP with ascorbate by inducing members of the *oxyR* regulon, including catalase and peroxidases (Fig. 11C, D), which is evidence for H_2O_2 production. The importance of this cellular response is illustrated by the fact that an *oxyR*-deficient mutant, unable to induce protection against H_2O_2, was highly sensitive to the combination of MnP and ascorbate; in the absence of ascorbate, the MnP did not cause any deleterious effects (Fig. 11B). The toxicity of the Mn(III) salen EUK-8 has also been attributed to the increased production of $O_2^{\bullet-}$ and H_2O_2 (78).
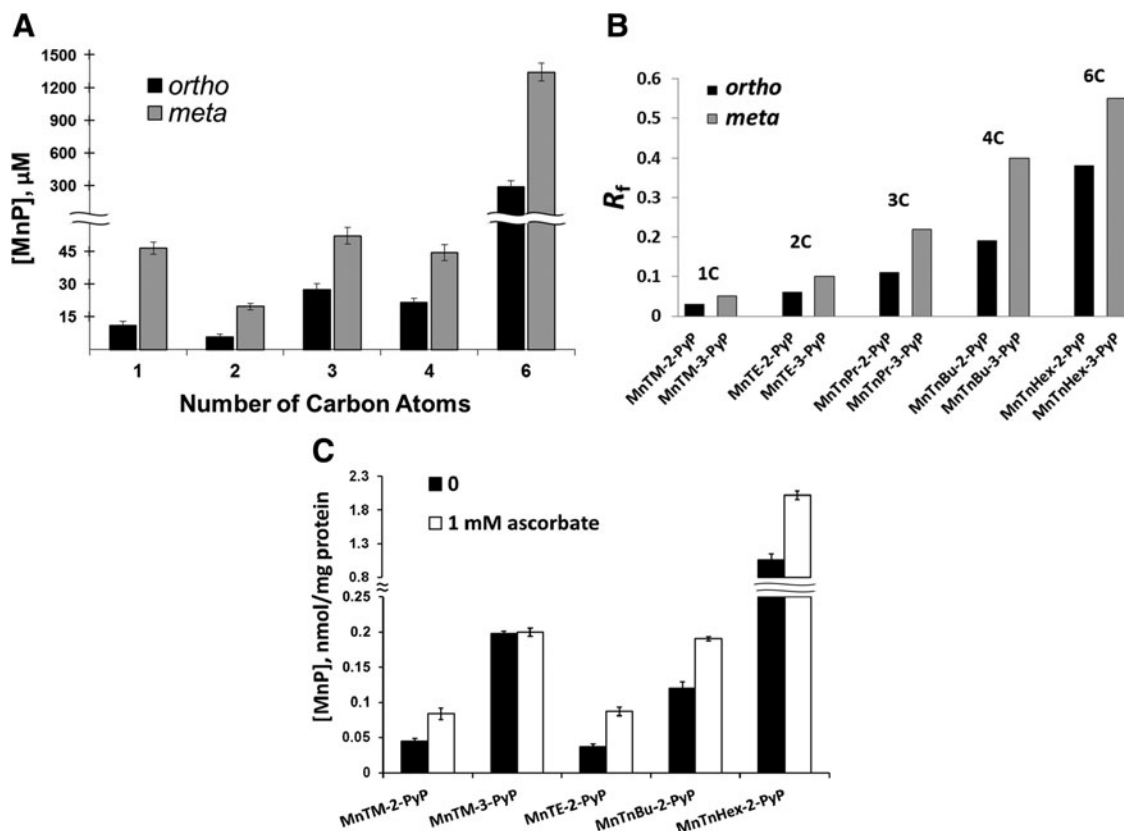

FIG. 10. Relationship between lipophilicity and cellular uptake of MnPs. **(A)** Accumulation of *ortho* and *meta* isomeric Mn(III) *meso*-tetrakis(*N*-alkylpyridyl)porphyrins in the cytosolic fractions of wild-type *E. coli* (AB1157) after 1 h of incubation with 5 μM Mn porphyrin (MnP) in M9CA medium. Bars represent mean ± SE. **(B)** Lipophilicity of *ortho* and *meta* isomeric MnPs defined by chromatographic retention factor, R_f. The R_f depends on the number of carbon atoms in alkylpyridyl chains of MnPs and correlates well with partition coefficient between n-octanol and water, P_{ow} (66,67). **(C)** Effect of ascorbate on MnP uptake. Wild-type *E. coli* (AB1157) was incubated for 1 h at 37°C in M9CA medium containing 5 μM Mn(III) *meso*-tetrakis(*N*-alkylpyridyl)porphyrins with or without 1 mM sodium ascorbate. Bars represent mean ± SE. SE, standard error.
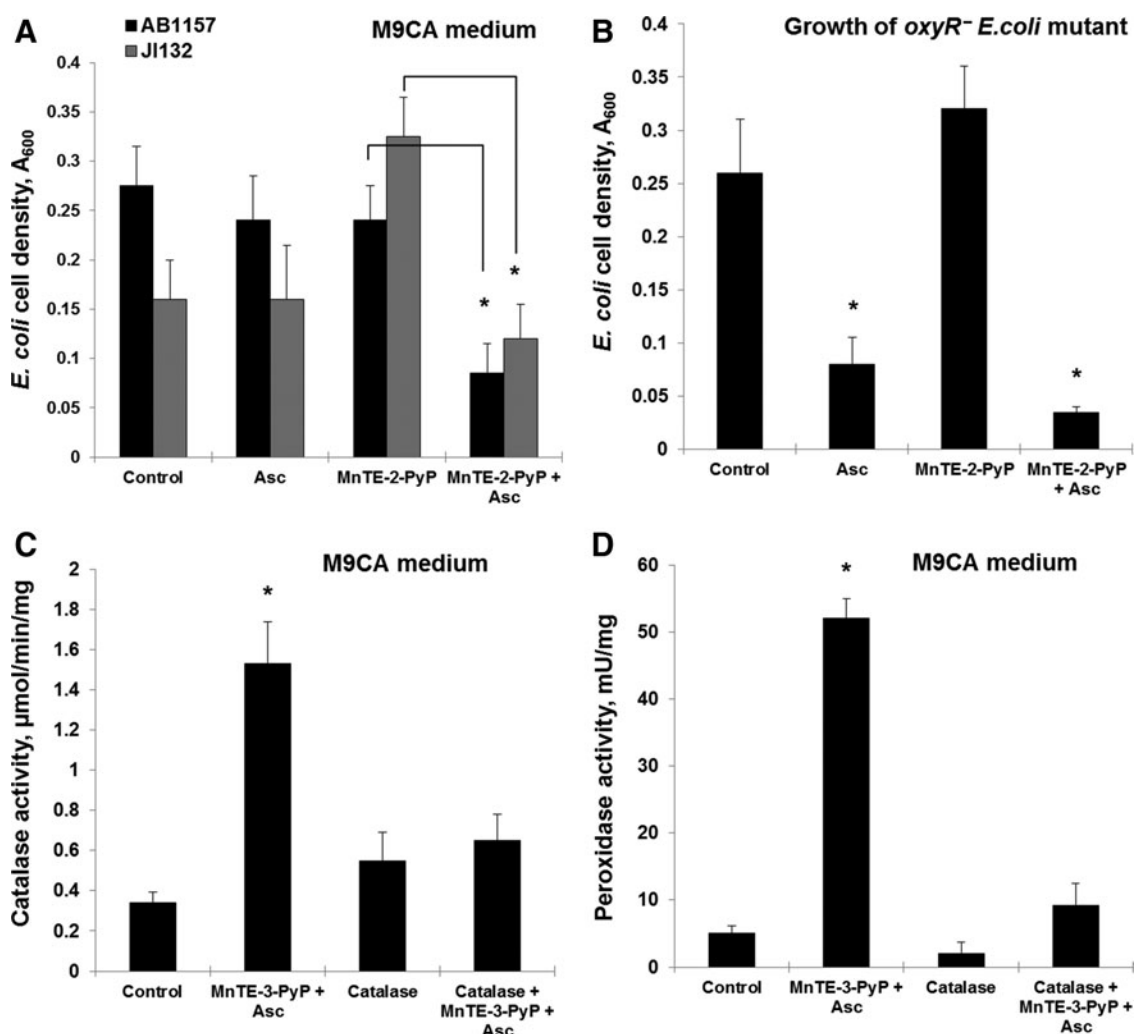
FIG. 11. **Ascorbate-dependent toxicity of MnTE-(2 and 3)-PyP. (A)** Suppression of *E. coli* growth by MnTE-2-PyP plus ascorbate (M9CA medium) **(B)**. Growth of *oxyR*-deficient *E. coli* mutant in the presence of MnTE-2-PyP plus ascorbate **(C, D)**; Induction of catalase and peroxidase. Adapted from ref. (15).

The *E. coli*-based discovery of MnP-ascorbate cytotoxicity (92) brought up the idea that the combination can be used for anticancer treatment (48,95,117,130). The therapeutic potential of pharmacological doses of ascorbate alone has already been demonstrated in several preclinical and clinical trials (46,61,83,127) and is based on the increased production of reactive species due to ascorbate oxidation, catalyzed by endogenous metalloproteins (36). MnPs, however, are advantageous, as their redox properties can be optimized in order to achieve the maximal rate of ascorbate oxidation. Consequently, a maximal production of H_2O_2 and other reactive species can be achieved, causing a more efficient tumor destruction. Promising results of such combinational catalytic therapy have been reported (48,95,130). *In vitro* experiments have shown that some cancer cell lines are more sensitive to either cationic MnPs or Fe porphyrins (FePs) alone and to the MnP-ascorbate combination than are normal cells (121). Among the reasons is preferential accumulation of porphyrins in neoplastic cells (51,72).

Toxicity of amphiphilic SOD mimics could be explained by the membrane damage due to the detergent-like action. Such

action, however, requires a high SOD mimic/lipid ratio (107) that cannot be achieved at the concentrations usually used. Further, no signs of membrane damage were detected when amphiphilic metalloporphyrins were tested at concentrations of approximately $50 \mu M$ (Benov *et al.*, unpublished observation). Since such compounds accumulate in cells to much higher concentrations than their hydrophilic analogs, their higher toxicity most probably results from blocking proteins/enzymes that require heme for their function (113).

Some toxicity of metalloporphyrin-based SOD mimics could be related to the light-dependent generation of ROS, mainly singlet oxygen, as demetallation of these compounds in the cytoplasm yields a photosensitizing metal-free porphyrin ligand *in situ*. Such compounds show much lower toxicity in the dark than when cultures are illuminated (96,121). Of note, MnPs and FePs are not photosensitizers *per se*, whereas their corresponding free ligands or the Zn analogues (ZnPs) have been explored as potent photosensitizers for photodynamic therapy (2–4,24,26,27).

Depending on the nature of the metalloporphyrin, its concentration, and the environment, including growth media

and cellular reductants, different mechanisms can eventually combine, leading to cell damage.

The strategies for decreasing the MnP toxicity

As mentioned earlier, the bioefficacy of amphiphilic MnP-based SOD mimics is limited by their higher toxicity. Further efforts have been directed toward decreasing the toxicity of SOD mimics while preserving the high SOD activity and lipophilicity. High catalytic activity was maintained by preserving the *ortho* cationic pyridyl nitrogens that dominate the thermodynamics and kinetics of metalloporphyrins-catalyzed $O_2^{\bullet-}$ dismutation. Previous investigations have shown that replacement of a CH_2 group in the butyl chain of MnTnBu-2-PyP[5+] with an oxygen atom diminishes its toxicity, but at the expense of decreased lipophilicity and, consequently, decreased cellular accumulation (20). Applying such a strategy to MnTnHex-2-PyP[5+] led to the synthesis of its methoxy analog, MnTMOHex-2-PyP[5+]. Its lipophilicity was, indeed, much lower than that of MnTnHex-2-PyP[5+]. Since *meta* isomers are more lipophilic than their *ortho* analogs (Fig. 10B), *meta* isomers of hexyl and ethyl species were synthesized and examined using *sodA sodB E. coli* (123). Both MnTMOHex-3-PyP[5+] and MnTMOE-3-PyP[5+] appeared more efficacious than MnTnHex-3-PyP[5+] and MnTE-3-PyP[5+] in supporting the aerobic growth of SOD-deficient *E. coli* (Fig. 12).

In an attempt to preserve the lipophilicity of alkoxyalkylated porphyrins, the oxygen atoms were pushed deeper into the cavity encircled by the *N*-alkylpyridyl substituents.

The reduced oxygen exposure to solvent prevented its solvation, and, thus, preserved the lipophilicity of the oxygenated derivatives. Such an optimized molecule, Mn(III) *meso*-tetrakis(*N*-n-butoxyethylpyridinium-2-yl)porphyrin (MnTnBuOE-2-PyP[5+]) was as lipophilic as its non-derivatized seven-carbon chain alkyl analog, MnTnHep-2-PyP[5+] and stimulated the aerobic growth of SOD-deficient *S. cerevisiae* (Fig. 13). At concentrations 5–30 μM, MnTnBuOE-2-PyP[5+] improved the aerobic growth of the *sod1Δ* yeast strain, whereas MnTnHep-2-PyP[5+] was toxic even at 5 μM (Fig. 13). The applicability of these results to higher organisms was tested in a mouse toxicity study, where MnTnBuOE-2-PyP[5+] was much less toxic than either MnTnHex-2-PyP[5+] or MnTnHep-2-PyP[5+] (93,123) [reviewed in detail in (120)].

The SOD mimics and E. coli growth curves

The growth pattern of most microorganisms in a closed habitat can be divided in three distinct phases: lag phase, during which the organisms adapt to the new environment and do not grow; exponential phase, where cell number increases in geometric progression; and stationary phase, where growth practically stops due to the lack of nutrients, accumulation of inhibitory products, or limit of space (90). Important information about the mechanism of action of tested compounds can be obtained by analyzing the kinetics of microbial growth. The significance of analyzing growth curves has been illustrated using the FeP-based SOD mimics. *Para* cationic Fe(III) *N*-methylpyridylporphyrin, FeTM-4-PyP[5+]
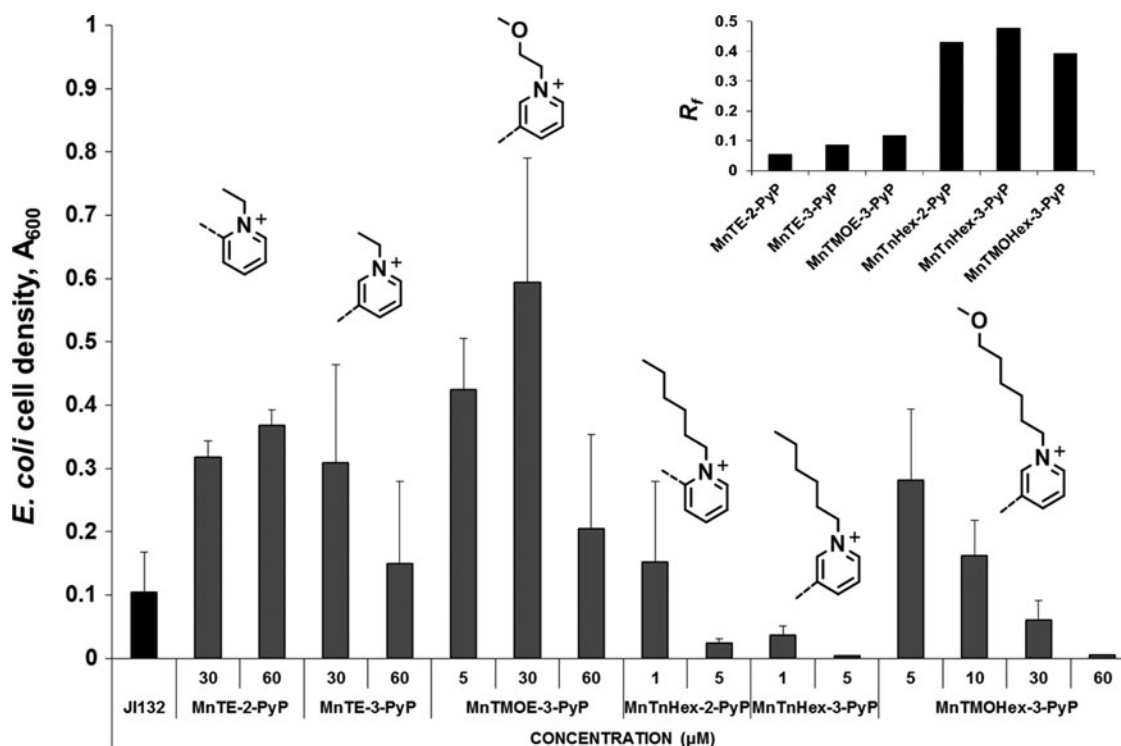

FIG. 12. Comparison of the efficacy/toxicity profiles of methoxy-derivatized cationic Mn(III) *N*-substituted pyridyl porphyrins (MnTMOE-3-PyP[5+] and MnTMOHex-3-PyP[5+]) with their respective alkyl analogs (*ortho* MnTE-2-PyP[5+], MnTnHex-2-PyP[5+] and *meta* MnTE-3-PyP[5+], MnTnHex-3-PyP[5+]). Growth of SOD-deficient *E. coli* strain (JI132) in five amino acid medium was followed turbidimetrically at 600 nm (123). Cell density at 16th hour of growth is shown. The *meta* ethyl has similar R_f as *meta* methoxyethyl, and the *meta* hexyl has R_f similar to *meta* methoxyhexyl (*inset*) (123).
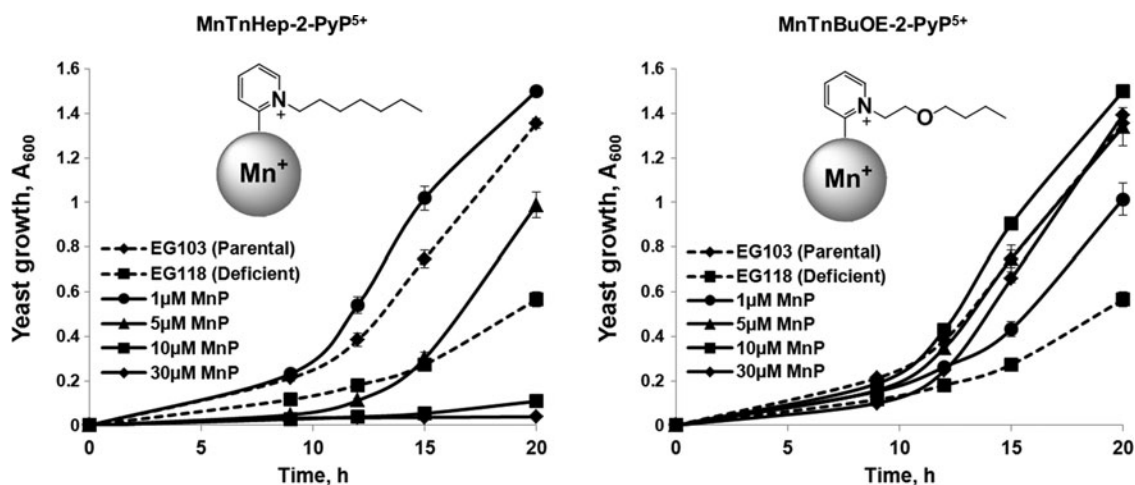
FIG. 13. Growth of wild-type (EG 103) and SOD-deficient (EG118, *sod1Δ*) *Saccharomyces cerevisiae* strains in the presence of MnTnHep-2-PyP^{5+} and MnTnBuOE-2-PyP^{5+} (1, 5, 10, or 30 μM). Cultures were grown in YPD medium, and growth was monitored turbidimetrically at 600 nm. Adapted from ref. (93).

reported in the late 1970s was the first metalloporphyrin to possess a high catalytic rate constant for $O_2^{\bullet -}$ dismutation [log $k_{cat}(O_2^{\bullet -}) = 7.20)$] (89). Based on the *ortho*-driven design of *N*-alkylpyridylporphyrins, FePs FP-15, WW-85, and INO-4885 have been synthesized. Beneficial effects of such FePs have been reported in various pathological conditions, including spinal cord injury, burn and smoke inhalation injury, septic shock, diabetes, and so on (57,68,79,80,91,115,116). The effect was attributed to the catalytic decomposition of peroxynitrite by FePs. Since Fe(III) *N*-alkylpyridylporphyrins have SOD activity that is very similar to their Mn analogs, as indicated by their log $k_{cat}(O_2^{\bullet -})$ values (19,122), the *in vivo* FeP-based protection could have ensued from both peroxynitrite decomposition and superoxide dismutation (17,120). Initially, the Fe(III) *N*-alkylpyridylporphyrins were tested on the *sodA*

sodB E. coli at a concentration optimal for the MnP analogs, 25 μM. Under such conditions, neither cationic nor anionic FePs (FeTM-2-PyP^{5+}, Fe^{III}TE-2-PyP^{5+}, Fe^{III}T(TMA)P^{5+}, Fe^{III}TCPP^{3-}, Fe^{III}T(TFTMA)P^{5+}, and Fe^{III}TSPP^{3-}) afforded protection; moreover, they acted as bacteriostatics to both SOD-deficient and SOD-proficient *E. coli* under aerobic and anaerobic conditions (19) (Fig. 14). At much lower concentrations, 0.01–1.0 μM, FePs stimulated the growth of the *sodA sodB E. coli* (Fig. 15). With FePs, however, the *sodA sodB* growth pattern was different than that of the SOD-containing and MnP-stimulated SOD-deficient cultures. If a compound substitutes for the SOD enzymes, then the SOD-deficient mutants should follow a growth pattern similar to that of the SOD-containing strains. As mentioned, both *sodA sodB E. coli* and *sod1Δ S. cerevisiae* can accumulate mutations that suppress the
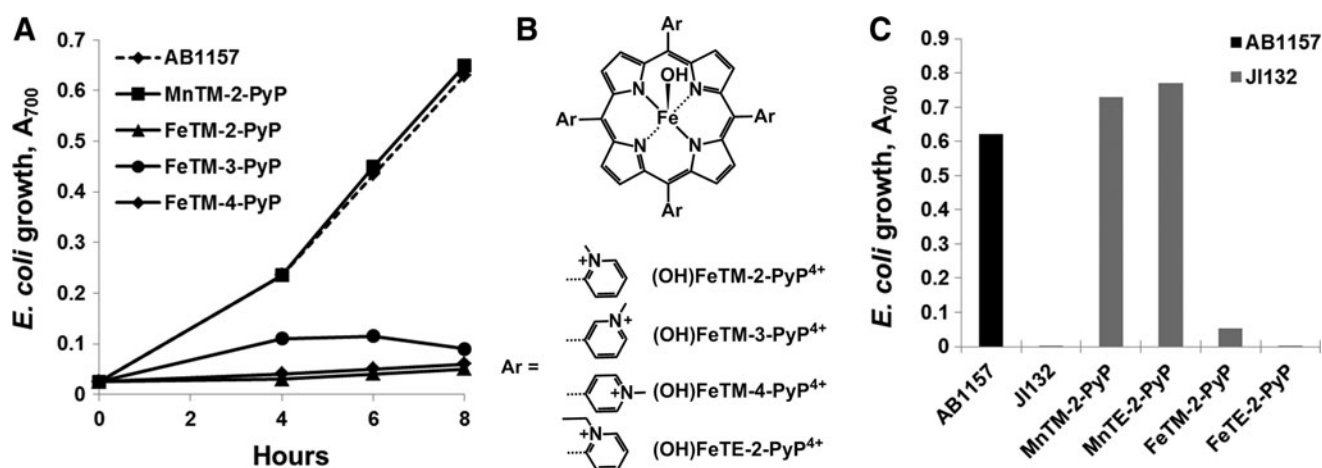

FIG. 14. Comparison between MnPs and FePs. (A) Growth of wild-type *E. coli* AB1157 in casamino acids (M9CA) medium in the presence of 25 μM of *ortho* (H$_2$O)MnTM-2-PyP^{5+}, or *ortho*, *meta*, and *para* (OH)FeTMPyP^{4+} under anaerobic conditions. The other axial ligand in MnPs and FePs is water molecule. Identical data were obtained with the JI132 SOD-deficient strain (not shown); anaerobically with and without MnTM-2-PyP^{5+} the SOD-deficient strain grows as well as wild type. **(B)** Structures of *ortho*, *meta*, and *para* (OH)FeTMPyP^{4+} and *ortho* (OH)FeTE-2-PyP^{5+}. **(C)** Effect of (H$_2$O)MnTM-2-PyP^{5+}, (H$_2$O)MnTE-2-PyP^{5+}, (OH)FeTM-2-PyP^{5+}, and (OH)FeTE-2-PyP^{5+} at 25 μM on the aerobic growth of SOD-deficient *E. coli* JI132 in 5AA medium. A_{700nm} after 56 h of growth is shown. Adapted from ref. (19).
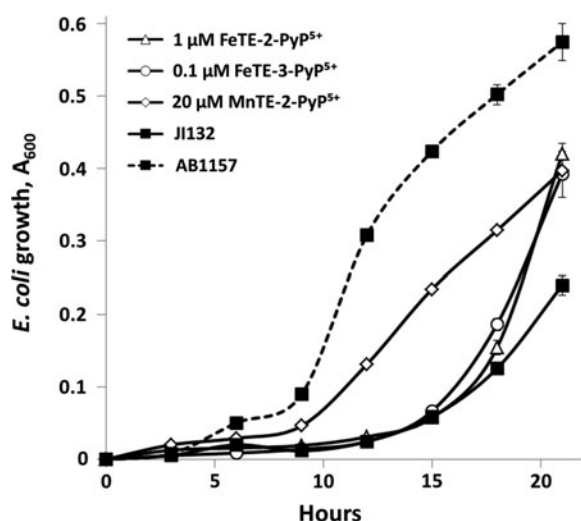
FIG. 15. **Growth of SOD-deficient JI132 and wild-type AB1157 *E. coli* in five-amino-acid medium in the presence of FePs and MnPs. FeP has essentially the same log $k_{cat}(O_2^{\bullet -})$ as MnP (17).** Adapted from (122).

aerobic defects, including the auxotrophies for amino acids (63,69). After prolonged incubation in restricted media, the SOD-deficient strains acquire the ability to overcome the auxotrophies and to restore growth without producing functional SODs. This is exhibited as a growth curve with a long lag followed by slow exponential growth. Some candidates for SOD mimics are able to act at this late stage and accelerate the growth rate of the *sodA sodB* cultures, without shortening the length of the lag phase. The growth stimulatory effect of FePs shown in Figure 15 could not be attributed to their SOD activity for two reasons: (i) Since FePs and MnPs have similar values of $k_{cat}(O_2^{\bullet -})$, the effect of FePs should have occurred at a concentration range at which analogous MnPs are efficacious. (ii) The growth curve of *sodA sodB* + FeP should be similar to the growth curve of parental *E. coli*. The data (122) indicate that at such low concentrations, FePs act in an identical way as simple Fe salts, thus supporting metabolism by providing Fe as an Fe source.

The sodA sodB E. coli versus the sod1Δ S. cerevisiae

A good strategy for screening the potential of SOD mimics is to compare their effects on *sodA sodB E. coli* and on *sod1Δ S. cerevisiae*. This strategy was used to screen the representatives from different classes of SOD mimics (85). Even though some of the tested compounds reportedly ameliorated oxidative stress in animal model systems, investigations of their ability to substitute for the missing cytoplasmic SODs produced unexpected results; only the Mn *N*-alkylpyridylporphyrin complexes MnTM-2-PyP^{5+}, MnTE-2-PyP^{5+}, and MnTM-4-PyP^{5+}, (the last one at low concentrations of $3\,\mu M$), stimulated the aerobic growth of SOD-deficient *E. coli* (85). MnTM-2-PyP^{5+} and MnTE-2-PyP^{5+} were also capable of supporting the aerobic growth of *sod1Δ S. cerevisiae*.

The two unicellular organisms responded differently to the same SOD mimic when other classes of compounds were studied. Thus, some compounds found to be efficient in rescuing the aerobic growth of the *sodA sodB E. coli* proved inefficient when tested in the *sod1Δ* yeast system. It has been hypothesized that such differences could be due either to the mislocalization or to the lack of sufficient concentration buildup of active species of these compounds in compartments where the radicals are present (85). For example, none of the Mn salen derivatives tested (Eukarion, EUK-134 and EUK-8) were efficient in *sod1Δ* yeast, but to a certain extent, improved the growth of *sodA sodB E. coli* (85). Since in Mn salen, chelated metal is weakly held (65), the growth stimulation could be due to Mn ions that dissociate from the ligands. It has been suggested that the protective action of Mn chelates could result from the facilitated import of Mn, which forms intracellular Mn complexes possessing SOD-like activity (1,6,7,10) and replaces the Fe in Fe-containing enzymes (5). The facilitated Mn transport may explain the beneficial effects of those SOD mimics that have low metal/ligand stability such as Mn salen and MnBr$_8$TSPP^{3-}. Although MnBr$_8$TSPP^{3-} is a poor SOD mimic, as indicated by its low log $k_{cat}(O_2^{\bullet -})$, its ability to protect SOD-deficient *E. coli* mirrored that of the potent mimic MnTM-2-PyP^{5+} (Fig. 16). It has been reported that in contrast to the stable MnP SOD mimics, which are found intact in the *E. coli* cytosol, cells loaded with MnBr$_8$TSPP^{3-} contained metal-free ligand (96). The following
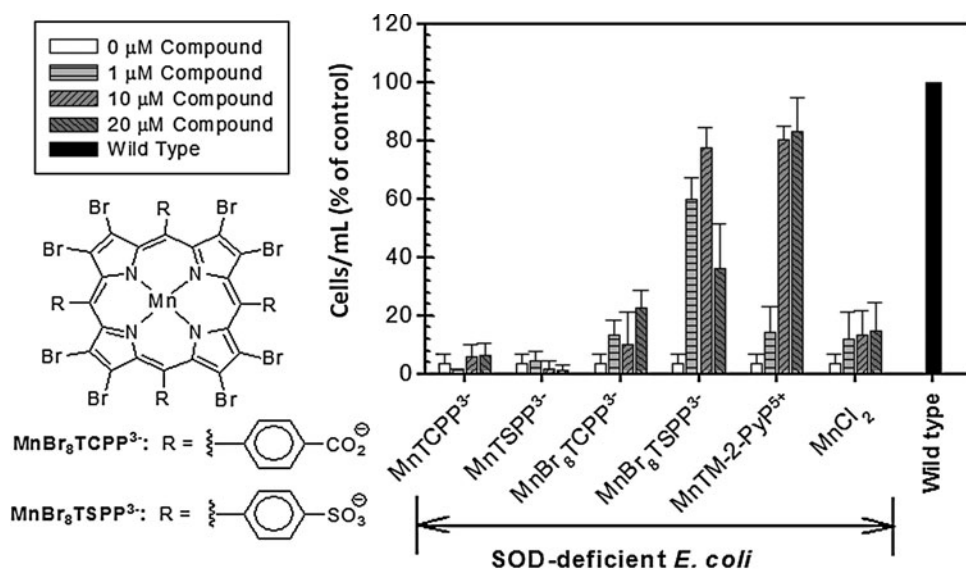

FIG. 16. **Effect of anionic β-brominated 4-sulfonatophenylporphyrin and its 4-carboxylatophenyl analog on the aerobic growth of SOD-deficient *E. coli* (JI132) in 5AA medium (data at 24th hour time point is presented).** MnTM-2-PyP^{5+} was used as a positive control. Results are presented as a percentage of the growth of the parental strain. Adapted from (96).
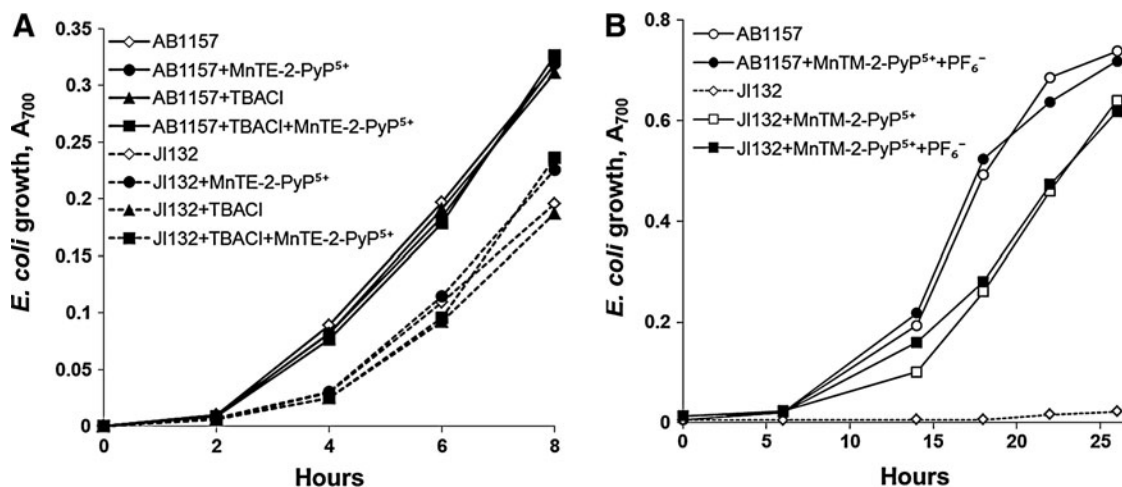
FIG. 17. **Testing the effect of chemicals used for preparation of SOD mimics.** Growth of SOD-deficient (JI132) and wild-type (AB1157) *E. coli* in the presence of: **(A)** TBACl in M9CA medium (Benov *et al.*, unpublished), **(B)** NH_4PF_6 (100), in five amino acid medium. Both compounds are used in the isolation and purification of cationic MnPs and, thus, may be present as impurities in final preparation. The compounds have been tested at the following concentrations: (i) TBACl, $20\,\mu M$; (ii) NH_4PF_6, $60\,\mu M$; (iii) MnTM-2-PyP^{5+}, $20\,\mu M$; and (iv) MnTE-2-PyP^{5+}, $1\,\mu M$. TBACl, tetra-n-butylammonium chloride; NH_4PF_6, ammonium hexafluorophosphate.

scenario was suggested to accommodate the spectroscopic and *E. coli* growth data: The Mn(III) complex is taken up by the cell and is reduced to its Mn(II) analog, which is then demetallated *in situ*, yielding Mn^{2+} and metal-free ligand. The nature of the resulting Mn^{2+} species inside the cell remains unknown, whereas the free ligand, exported out of the cell, is found in the medium. No demetallation was observed in a cell-free medium. Therefore, $MnBr_8TSPP^{3-}$ was protecting the SOD-deficient cells not by scavenging superoxide but by facilitating the Mn import. A study using *Criptococcus neoformans* suggests that Mn salen (EUK-8) is also acting as a Mn carrier (58). A similar effect of Mn was reported for *sod1Δ S. cerevisiae* (106), which implies that growth stimulation by the unstable Mn-based compounds might simply reflect their ability to transport manganese.

The purity of the tested compounds

Various commercial SOD mimics contain impurities, which can affect the outcomes of biological trials. Impurities are probably the main reason behind the contradictory reports about the bioefficacy of $MnTBAP^{3-}$ (98,99). Impure preparations of MnTE-2-PyP^{5+} obtained from CalBiochem (containing ∼25% tetraethylated MnTE-2-PyP^{5+}; the remaining

∼75% comprised tri-, di-, monoethylated, and non-ethylated derivatives) (99) may be a reason for the lower-than-anticipated efficacy of this SOD mimic, when tested on SOD-deficient *E. coli* and *S. cerevisiae* (85). Chemicals used in the preparation of SOD mimics, traces of which might remain in the final product, should also be tested for their biological activity. For example, neither tetra-n-butylammonium chloride nor ammonium hexafluorophosphate, used in the preparation of MnP-based SOD mimics caused any adverse effects when tested on *E. coli* (100) (Fig. 17). It is also important to quantify the amount of residual metal (Mn, Fe, *etc.*) present in the preparations (97), and to assess the biological effect of respective metal salts at matching concentrations.

The role of SOD-deficient E. coli and S. cerevisiae in distinguishing SOD mimics from non-SOD mimics

Various metal- or non-metal-based compounds (Fig. 18) were reportedly capable of suppressing oxidative stress in animal models: Mn(III) salen derivatives, such as EUK-8 (45,103); Mn(II) cyclic polyamine/azacrown ethers, such as M40403 (102); nitrones, such as NXY-059 (53); nitroxides, such as tempol (17,110); and $MnTBAP^{3-}$ (73,128). When tested on SOD-deficient *E. coli* or *S. cerevisiae*, none of them acted as

FIG. 18. **Structures of various classes of compounds that have been tested as SOD mimics.** Summarized in (17,82).
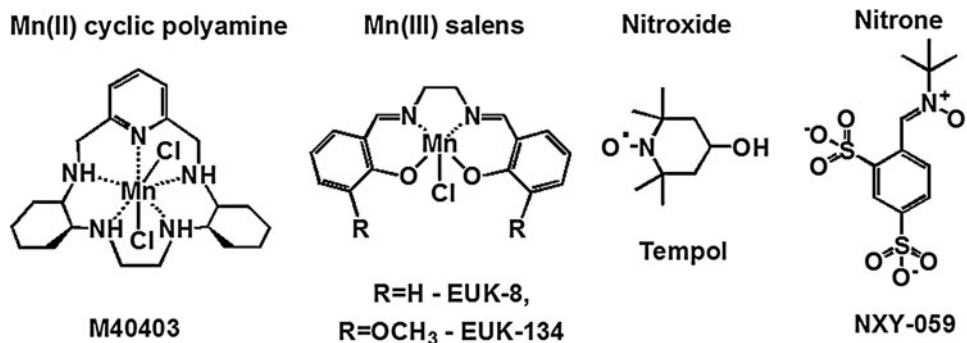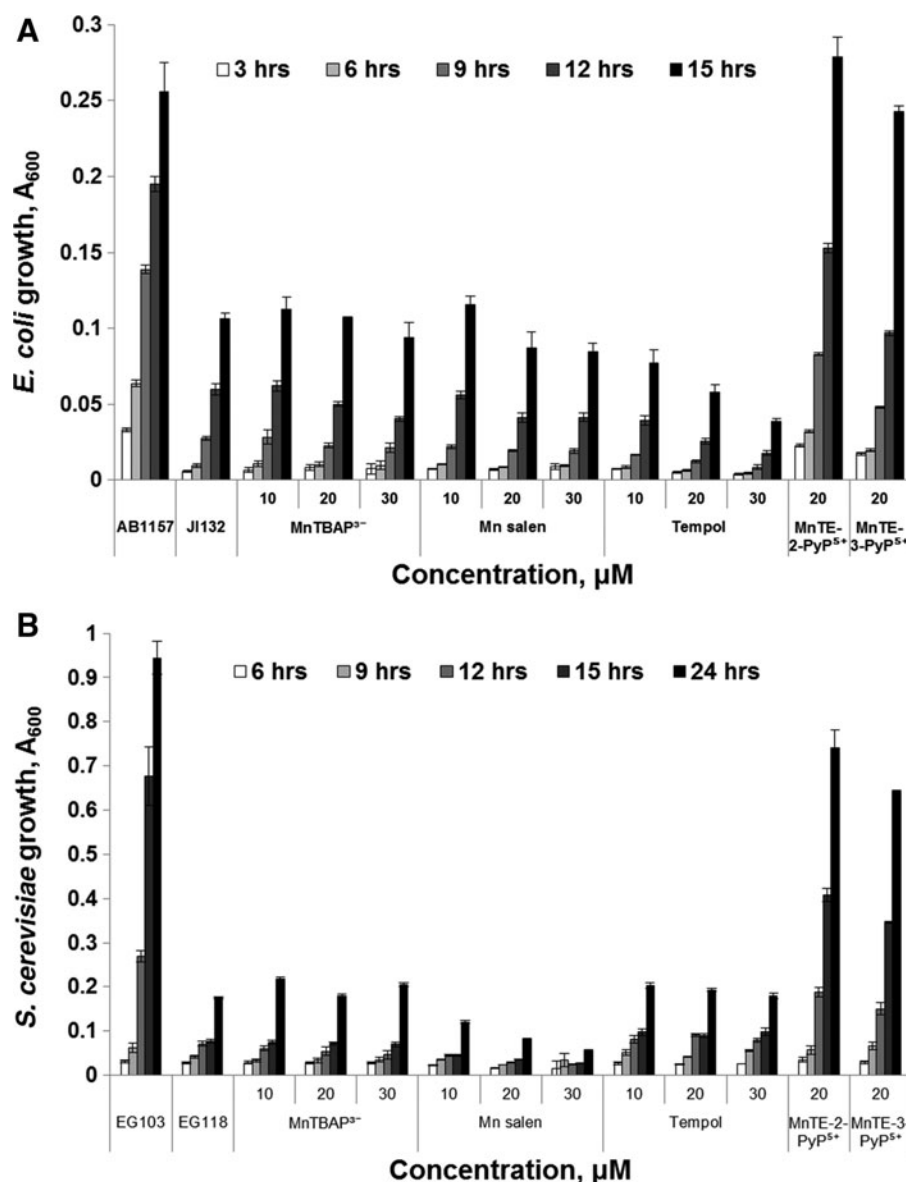
FIG. 19. Growth of *E. coli* and *S. cerevisiae* in the presence of different redox-active compounds and SOD mimics. Wild-type AB1157 and SOD-deficient JI132 *E. coli* **(A)** were grown in five amino acid medium. Wild-type EG103 and SOD1-deficient EG118 *S. cerevisiae* strains **(B)** were grown in YPD medium. Growth was monitored turbidimetrically at 600 nm. Adapted from (13) (Benov *et al.*, unpublished). Similar results were reported by Munroe *et al.* (85).

SOD mimics (Figs. 19 and 20). Such results are not unexpected, because the log $k_{cat}(O_2^{\bullet -})$ of some of those compounds is lower than the rate constant of spontaneous $O_2^{\bullet -}$ dismutation ($5 \times 10^5 \, M^{-1} \cdot s^{-1}$), while the others have a high log $k_{cat}(O_2^{\bullet -})$ (M40403, EUK-8), but are unstable and eventually decompose and lose the redox-active metal. In a comprehensive study, Munroe and coworkers reported that EUK-8 and EUK-134 at concentrations of approximately 100 μM improved the growth of the *sodA sod B E. coli*, but the effect was similar to that of Mn(II)EDTA^{2-} or MnCl$_2$ (85). None of the two Mn salen compounds improved the growth of the *sod1Δ S. cerevisiae* (85). No positive results were reported for M40403 (85). Since all these compounds are redox active, they most probably act by mechanisms other than catalysis of $O_2^{\bullet -}$ dismutation (17,82,104).

Concluding Remarks

Results obtained so far support the benefit of using SOD-deficient unicellular organisms for predicting the therapeutic potential of artificial SOD substitutes and for studying the mechanisms of action of redox-active compounds. The absence of superoxide-scavenging enzymes in these organisms offers an unambiguous background for testing *in vivo* the superoxide-scavenging capacity of SOD mimics. Such simple systems allow growth conditions and growth media to be manipulated, which is crucial for studying the mechanisms of action and, to some extent, the biological transformations of newly synthesized compounds. The relative simplicity of *E. coli* and *S. cerevisiae* is essential in the exploration of factors that affect accumulation and subcellular distribution of various types of compounds. Information on the impact of stability, charge, lipophilicity, size, shape, and bulkiness of molecules on the uptake and subcellular distribution of redox-active compounds could be obtained using these unicellular organisms. No less important, knowledge obtained with *E. coli* and *S. cerevisiae* could be successfully translated to higher organisms. Application of SOD-deficient *E. coli* and *S. cerevisiae* models proved that compounds with low catalytic rate constants (k_{cat}) for $O_2^{\bullet -}$ dismutation and unsuitable
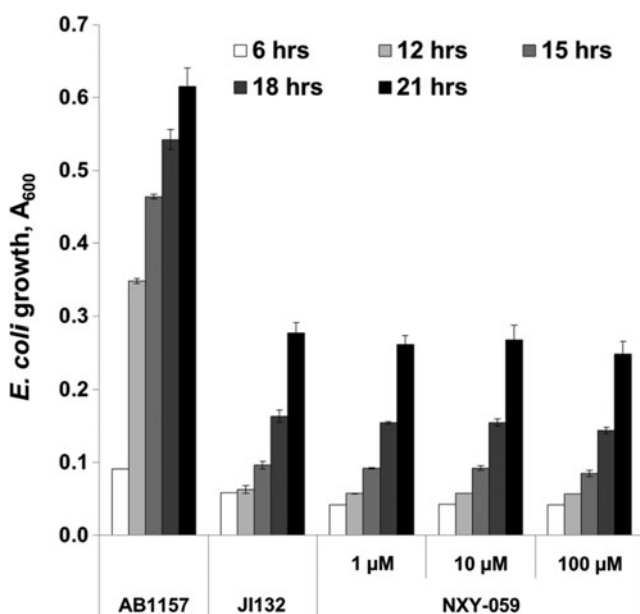
FIG. 20. Effect of nitrone, NXY-059 on the growth of SOD-deficient *E. coli* (JI132) in five amino acid medium (Benov *et al.*, unpublished). NXY-059 has been widely tested in animal models of oxidative stress with fair success, but failed in the clinical trials on stroke patients (44,109).

reduction potentials ($E_{1/2}$) cannot act *in vivo* as SOD mimics, and indicate that the beneficial effects observed in various animal model systems most probably result from activities other than the removal of $O_2^{\bullet-}$. High catalytic constant, however, is not a sufficient predictor of an SOD mimic's bioefficacy. Stability, size, shape, charges, lipophilicity, and other intrinsic properties of the molecule, which affect cellular uptake, subcellular distribution, and biological transformations, are factors that can outweigh the impact of k_{cat} and should be tested on relevant biological systems before a compound is identified as an SOD mimic. It is important to keep in mind that irrespective of their apparent simplicity, the *E. coli* and *S. cerevisiae* microorganisms have complex physiology and metabolism, and interpretation of their responses to externally added compounds is not straightforward. Various factors, including composition of the growth media, aeration, physiological state of the initial inoculum, time of incubation, and even illumination, could affect cellular response and should be taken into consideration when results are analyzed. It becomes clear that a compound should not be recognized as an SOD mimic based on the results obtained only in one model system, and that a thorough investigation of biological actions other than superoxide scavenging should be carried out.

Acknowledgments

References

1. Al-Maghrebi M, Fridovich I, and Benov L. Manganese supplementation relieves the phenotypic deficits seen in superoxide-dismutase-null *Escherichia coli*. *Arch Biochem Biophys* 402: 104–109, 2002.
2. Al-Mutairi DA, Craik JD, Batinic-Haberle I, and Benov LT. Photosensitizing action of isomeric zinc N-methylpyridylporphyrins in human carcinoma cells. *Free Radic Res* 40: 477–483, 2006.
3. Al-Mutairi DA, Craik JD, Batinic-Haberle I, and Benov LT. Inactivation of metabolic enzymes by photo-treatment with zinc meta N-methylpyridylporphyrin. *Biochim Biophys Acta* 1770: 1520–1527, 2007.
4. Al-Mutairi DA, Craik JD, Batinic-Haberle I, and Benov LT. Induction of oxidative cell damage by photo-treatment with zinc N-methylpyridylporphyrin. *Free Radic Res* 41: 89–96, 2007.
5. Anjem A, and Imlay JA. Mononuclear iron enzymes are primary targets of hydrogen peroxide stress. *J Biol Chem* 287: 15544–15556, 2012.
6. Archibald FS, and Fridovich I. Manganese and defenses against oxygen toxicity in *Lactobacillus plantarum*. *J Bacteriol* 145: 442–451, 1981.
7. Archibald FS, and Fridovich I. The scavenging of superoxide radical by manganous complexes: *in vitro*. *Arch Biochem Biophys* 214: 452–463, 1982.
8. Bafana A, Dutt S, Kumar A, Kumar S, and Ahuja PS. The basic and applied aspects of superoxide dismutase. *J Mol Catal B: Enzymatic* 68: 129–138, 2011.
9. Bafana A, Dutt S, Kumar S, and Ahuja PS. Superoxide dismutase: an industrial perspective. *Crit Rev Biotechnol* 31: 65–76, 2011.
10. Barnese K, Gralla E, Valentine J, and Cabelli DE. Biologically relevant mechanism for catalytic superoxide removal by simple manganese compounds. *Proc Natl Acad Sci U S A* 109: 6892–6897, 2012.
11. Batinic-Haberle I, Reboucas JS, Benov L, and Spasojevi I. Chemistry, biology and medical effects of water soluble metalloporphyrins. In: *Handbook of Porphyrin Science*, edited by Kadish KM, Smith KM, and Guillard R. Singapore: World Scientific, 2011, pp. 291–393.
12. Batinic-Haberle I, Benov L, Spasojevic I, and Fridovich I. The ortho effect makes manganese(III) meso-tetrakis(N-methylpyridinium-2-yl)porphyrin a powerful and potentially useful superoxide dismutase mimic. *J Biol Chem* 273: 24521–24528, 1998.
13. Batinic-Haberle I, Cuzzocrea S, Rebouças JS, Ferrer-Sueta G, Mazzon E, Di Paola R, Radi R, Spasojevic I, Benov L, and Salvemini D. Pure MnTBAP selectively scavenges peroxynitrite over superoxide: comparison of pure and commercial MnTBAP samples to MnTE-2-PyP in two models of oxidative stress injury, an SOD-specific *Escherichia coli* model and carrageenan-induced pleurisy. *Free Radic Biol Med* 46: 192–201, 2009.
14. Batinic-Haberle I, Liochev SI, Spasojevic I, and Fridovich I. A potent superoxide dismutase mimic: manganese beta-octabromo-meso-tetrakis-(N-methylpyridinium-4-yl) porphyrin. *Arch Biochem Biophys* 343: 225–233, 1997.
15. Batinić-Haberle I, Rajić Z, and Benov L. A combination of two antioxidants (an SOD mimic and ascorbate) produces a pro-oxidative effect forcing *Escherichia coli* to adapt via

induction of oxyR regulon. *Anticancer Agents Med Chem* 11: 329–340, 2011.

16. Batinic-Haberle I, Rajic Z, Tovmasyan A, Reboucas JS, Ye X, Leong KW, Dewhirst MW, Vujaskovic Z, Benov L, and Spasojevic I. Diverse functions of cationic Mn(III) N-substituted pyridylporphyrins, recognized as SOD mimics. *Free Radic Biol Med* 51: 1035–1053, 2011.

17. Batinić-Haberle I, Rebouças JS, and Spasojević I. Superoxide dismutase mimics: chemistry, pharmacology, and therapeutic potential. *Antioxid Redox Signal* 13: 877–918, 2010.

18. Batinic-Haberle I, Spasojevic I, and Fridovich I. Tetrahydrobiopterin rapidly reduces the SOD mimic Mn(III) ortho-tetrakis(N-ethylpyridinium-2-yl)porphyrin. *Free Radic Biol Med* 37: 367–374, 2004.

19. Batinic-Haberle I, Spasojevic I, Hambright P, Benov L, Cmmbliss AL, and Fridovich I. Relationship among redox potentials, proton dissociation constants of pyrrolic nitrogens, and *in vivo* and *in vitro* superoxide dismutating activities of manganese(III) and iron(III) water-soluble porphyrins. *Inorg Chem* 38: 4011–4022, 1999.

20. Batinic-Haberle I, Spasojevic I, Stevens RD, Hambright P, Neta P, Okado-Matsumoto A, and Fridovich I. New class of potent catalysts of $O_2^{\bullet-}$ dismutation: Mn(III) ortho-methoxyethylpyridyl- and di-ortho-methoxyethylimidazolylporphyrins. *Dalton Trans* 1696–1702, 2004.

21. Batinic-Haberle I, Spasojevic I, Tse HM, Tovmasyan A, Rajic Z, St Clair DK, Vujaskovic Z, Dewhirst MW, and Piganelli JD. Design of Mn porphyrins for treating oxidative stress injuries and their redox-based regulation of cellular transcriptional activities. *Amino Acids* 42: 95–113, 2012.

22. Batinic-Haberle I, Tovmasyan A, Roberts ERH, Vujaskovic Z, Leong KW, and Spasojevic I. SOD therapeutics: latest insights into their structure-activity relationships and impact on the cellular redox-based signaling pathways. *Antioxid Redox Signal* 20: 2372–2415, 2014.

23. Benatar M. Lost in translation: treatment trials in the SOD1 mouse and in human ALS. *Neurobiol Dis* 26: 1–13, 2007.

24. Benov L, Batinic-Haberle I, Spasojevic I, and Fridovich I. Isomeric N-alkylpyridylporphyrins and their Zn(II) complexes: inactive as SOD mimics but powerful photosensitizers. *Arch Biochem Biophys* 402: 159–165, 2002.

25. Benov L, Chang LY, Day B, and Fridovich I. Copper, zinc superoxide dismutase in *Escherichia coli* periplasmic localization. *Arch Biochem Biophys* 319: 508–511, 1995.

26. Benov L, Craik J, and Batinic-Haberle I. The potential of Zn(II) N-alkylpyridylporphyrins for anticancer therapy. *Anticancer Agents Med Chem* 11: 233–241, 2011.

27. Benov L, Craik J, and Batinic-Haberle I. Protein damage by photo-activated Zn(II) N-alkylpyridylporphyrins. *Amino Acids* 42: 117–128, 2012.

28. Benov L, and Fridovich I. Superoxide dismutase protects against aerobic heat shock in *Escherichia coli*. *J Bacteriol* 177: 3344–3346, 1995.

29. Benov L, and Fridovich I. The rate of adaptive mutagenesis in *Escherichia coli* is enhanced by oxygen (superoxide). *Mutat Res* 357: 231–236, 1996.

30. Benov L, and Fridovich I. Why superoxide imposes an aromatic amino acid auxotrophy on *Escherichia coli*: the transketolase connection. *J Biol Chem* 274: 4202–4206, 1999.

31. Benov L, Kredich NM, and Fridovich I. The mechanism of the auxotrophy for sulfur-containing amino acids imposed

upon *Escherichia coli* by superoxide. *J Biol Chem* 271: 21037–21040, 1996.

32. Benov LT, and Fridovich I. *Escherichia coli* expresses a copper- and zinc-containing superoxide dismutase. *J Biol Chem* 269: 25310–25314, 1994.

33. Bernard AS, Giroud C, Ching HYV, Meunier A, Ambike V, Amatore C, Collignon MG, Lemaître F, and Policar C. Evaluation of the anti-oxidant properties of a SOD-mimic Mn-complex in activated macrophages. *Dalton Trans* 41: 6399–6403, 2012.

34. Bilinski T, Krawiec Z, Liczmanski A, and Litwinska J. Is hydroxyl radical generated by the Fenton reaction in vivo? *Biochem Biophys Res Commun* 130: 533–539, 1985.

35. Carlioz A, and Touati D. Isolation of superoxide dismutase mutants in *Escherichia coli*: is superoxide dismutase necessary for aerobic life? *EMBO J* 5: 623–630, 1986.

36. Chen Q, Espey MG, Sun AY, Pooput C, Kirk KL, Krishna MC, Khosh DS, Drisko J, and Levine M. Pharmacologic doses of ascorbate act as a prooxidant and decrease growth of aggressive tumor xenografts in mice. *Proc Natl Acad Sci U S A* 105: 11105–11109, 2008.

37. Chiang SM, and Schellhorn HE. Regulators of oxidative stress response genes in *Escherichia coli* and their functional conservation in bacteria. *Arch Biochem Biophys* 525: 161–169, 2012.

38. Contestabile A. Amyotrophic lateral sclerosis: from research to therapeutic attempts and therapeutic perspectives. *Curr Med Chem* 18: 5655–5665, 2011.

39. Czapski G, and Goldstein S. The uniqueness of superoxide dismutase (SOD)—why cannot most copper compounds substitute SOD in vivo? *Free Radic Res Commun* 4: 225–229, 1988.

40. Czapski G, and Goldstein S. Requirements for SOD mimics operating *in vitro* to work also *in vivo*. *Free Radic Res Commun* 12–13 Pt 1: 167–171, 1991.

41. De Freitas JM, Liba A, Meneghini R, Valentine JS, and Gralla EB. Yeast lacking Cu-Zn superoxide dismutase show altered iron homeostasis: role of oxidative stress in iron metabolism. *J Biol Chem* 275: 11645–11649, 2000.

42. DeFreitas-Silva G, Reboucas JS, Spasojevic I, Benov L, Idemori YM, and Batinic-Haberle I. SOD-like activity of Mn(II) *β*-octabromo-meso-tetrakis(N-methylpyridinium-3-yl)porphyrin equals that of the enzyme itself. *Arch Biochem Biophys* 477: 105–112, 2008.

43. Delmastro-Greenwood MM, Tse HM, and Piganelli JD. Effects of metalloporphyrins on reducing inflammation and autoimmunity. *Antioxid Redox Signal* 20: 2465–2477, 2014.

44. Diener HC, Lees KR, Lyden P, Grotta J, Davalos A, Davis SM, Shuaib A, Ashwood T, Wasiewski W, Alderfer V, Hårdemark HG, and Rodichok L. NXY-059 for the treatment of acute stroke: pooled analysis of the SAINT I and II trials. *Stroke* 39: 1751–1758, 2008.

45. Doctrow SR, Baudry M, Huffman K, Malfroy B, and Melov S. Salen manganese complexes: multifunctional catalytic antioxidants protective in models for neurodegenerative diseases of aging in medicinal inorganic chemistry. In: *American Chemical Society Symposium Series 903, ACS*, edited by Sessler J, Doctrow SR, McMurry T, and Lippard S. Oxford University Press, 2005, pp. 319–347.

46. Du J, Martin SM, Levine M, Wagner BA, Buettner GR, Wang S-h, Taghiyev AF, Du C, Knudson CM, and Cullen JJ. Mechanisms of ascorbate-induced cytotoxicity in pancreatic cancer. *Clin Cancer Res* 16: 509–520, 2010.

47. Edsmyr F, and Menander-Huber KB. Orgotein efficacy in ameliorating side effects due to radiation therapy. *Eur J Rheumatol Inflamm* 4: 228–236, 1981.

48. Evans MK, Tovmasyan A, Batinic-Haberle I, and Devi GR. Mn porphyrin in combination with ascorbate acts as a pro-oxidant and mediates caspase-independent cancer cell death. *Free Radic Biol Med*, 2013 (in press).

49. Farr SB, D'Ari R, and Touati D. Oxygen-dependent mutagenesis in *Escherichia coli* lacking superoxide dismutase. *Proc Natl Acad Sci U S A* 83: 8268–8272, 1986.

50. Faulkner KM, Liochev SI, and Fridovich I. Stable Mn(III) porphyrins mimic superoxide dismutase *in vitro* and substitute for it *in vivo*. *J Biol Chem* 269: 23471–23476, 1994.

51. Figge FH, Weiland GS, and Manganiello LO. Cancer detection and therapy: affinity of neoplastic, embryonic, and traumatized tissues for porphyrins and metalloporphyrins. *Proc Soc Exp Biol Med* 68: 640, 1948.

52. Floyd RA, Castro Faria Neto HC, Zimmerman GA, Hensley K, and Towner RA. Nitrone-based therapeutics for neurodegenerative diseases: their use alone or in combination with lanthionines. *Free Radic Biol Med* 62: 145–156, 2013.

53. Floyd RA, Chandru HK, He T, and Towner R. Anti-cancer activity of nitrones and observations on mechanism of action. *Anticancer Agents Med Chem* 11: 373–379, 2011.

54. Floyd RA, Towner RA, He T, Hensley K, and Maples KR. Translational research involving oxidative stress and diseases of aging. *Free Radic Biol Med* 51: 931–941, 2011.

55. Fridovich I. Oxygen toxicity: a radical explanation. *J Exp Biol* 201: 1203–1209, 1998.

56. Fridovich I. Oxygen: how do we stand it? *Med Princ Pract* 22: 131–137, 2013.

57. Genovese T, Mazzon E, Esposito E, Di Paola R, Murthy K, Neville L, Bramanti P, and Cuzzocrea S. Effects of a metalloporphyrinic peroxynitrite decomposition catalyst, ww-85, in a mouse model of spinal cord injury. *Free Radic Res* 43: 631–645, 2009.

58. Giles SS, Batinic-Haberle I, Perfect JR, and Cox GM. *Cryptococcus neoformans* mitochondrial superoxide dismutase: an essential link between antioxidant function and high-temperature growth. *Eukaryot Cell* 4: 46–54, 2005.

59. Gort AS, and Imlay JA. Balance between endogenous superoxide stress and antioxidant defenses. *J Bacteriol* 180: 1402–1410, 1998.

60. Gralla EB, and Valentine JS. Null mutants of *Saccharomyces cerevisiae* Cu,Zn superoxide dismutase: characterization and spontaneous mutation rates. *J Bacteriol* 173: 5918–5920, 1991.

61. Hoffer LJ, Levine M, Assouline S, Melnychuk D, Padayatty SJ, Rosadiuk K, Rousseau C, Robitaille L, and Miller Jr WH. Phase I clinical trial of i.v. ascorbic acid in advanced malignancy. *Ann Oncol* 19: 1969–1974, 2008.

62. Imlay JA. Cellular defenses against superoxide and hydrogen peroxide. *Annu Rev Biochem* 77: 755–776, 2008.

63. Imlay JA, and Fridovich I. Isolation and genetic analysis of a mutation that suppresses the auxotrophies of superoxide dismutase-deficient *Escherichia coli* K12. *Mol Gen Genet* 228: 410–416, 1991.

64. Imlay JA, and Fridovich I. Suppression of oxidative envelope damage by pseudoreversion of a superoxide dismutase-deficient mutant of *Escherichia coli*. *J Bacteriol* 174: 953–961, 1992.

65. Keaney M, Matthijssens F, Sharpe M, Vanfleteren J, and Gems D. Superoxide dismutase mimetics elevate superox-

ide dismutase activity *in vivo* but do not retard aging in the nematode *Caenorhabditis elegans*. *Free Radic Biol Med* 37: 239–250, 2004.

66. Kos I, Benov L, Spasojević I, Rebouças JS, and Batinić-Haberle I. High lipophilicity of meta Mn(III) N-alkylpyridylporphyrin-based superoxide dismutase mimics compensates for their lower antioxidant potency and makes them as effective as ortho analogues in protecting superoxide dismutase-deficient *Escherichia coli*. *J Med Chem* 52: 7868–7872, 2009.

67. Kos I, Rebouças JS, DeFreitas-Silva G, Salvemini D, Vujaskovic Z, Dewhirst MW, Spasojević I, and Batinić-Haberle I. Lipophilicity of potent porphyrin-based antioxidants: comparison of ortho and meta isomers of Mn(III) N-alkylpyridylporphyrins. *Free Radic Biol Med* 47: 72–78, 2009.

68. Lange M, Szabo C, Enkhbaatar P, Connelly R, Horvath E, Hamahata A, Cox RA, Esechie A, Nakano Y, Traber LD, Herndon DN, and Traber DL. Beneficial pulmonary effects of a metalloporphyrinic peroxynitrite decomposition catalyst in burn and smoke inhalation injury. *Am J Physiol Lung Cell Mol Physiol* 300: L167–L175, 2011.

69. Lapinskas PJ, Cunningham KW, Xiu Fen L, Fink GR, and Culotta VC. Mutations in PMR1 suppress oxidative damage in yeast cells lacking superoxide dismutase. *Mol Cell Biol* 15: 1382–1388, 1995.

70. Lin SJ, and Culotta VC. The ATX1 gene of *Saccharomyces cerevisiae* encodes a small metal homeostasis factor that protects cells against reactive oxygen toxicity. *Proc Natl Acad Sci U S A* 92: 3784–3788, 1995.

71. Liochev SI. The mechanism of "Fenton-like" reactions and their importance for biological systems: a biologist's view. *Met Ions Biol Syst* 36: 1–39, 1999.

72. Lipson RL, Baldes EJ, and Gray MJ. Hematoporphyrin derivative for detection and management of cancer. *Cancer* 20: 2255–2257, 1967.

73. Liu D, Shan Y, Valluru L, and Bao F. Mn (III) tetrakis (4-benzoic acid) porphyrin scavenges reactive species, reduces oxidative stress, and improves functional recovery after experimental spinal cord injury in rats: comparison with methylprednisolone. *BMC Neurosci* 14: 23, 2013.

74. Liu XF, and Culotta VC. The requirement for yeast superoxide dismutase is bypassed through mutations in BSD2, a novel metal homeostasis gene. *Mol Cell Biol* 14: 7037–7045, 1994.

75. Longo VD, Gralla EB, and Valentine JS. Superoxide dismutase activity is essential for stationary phase survival in *Saccharomyces cerevisiae*: mitochondrial production of toxic oxygen species *in vivo*. *J Biol Chem* 271: 12275–12280, 1996.

76. Lyden PD, Shuaib A, Lees KR, Davalos A, Davis SM, Diener HC, Grotta JC, Ashwood TJ, Hardemark HG, Svensson HH, Rodichok L, Wasiewski WW, and Åhlberg G. Safety and tolerability of NXY-059 for acute intracerebral hemorrhage: the CHANT trial. *Stroke* 38: 2262–2269, 2007.

77. Macomber L, Rensing C, and Imlay JA. Intracellular copper does not catalyze the formation of oxidative DNA damage in *Escherichia coli*. *J Bacteriol* 189: 1616–1626, 2007.

78. Matthijssens F, Back P, Braeckman BP, and Vanfleteren JR. Prooxidant activity of the superoxide dismutase (SOD)-mimetic EUK-8 in proliferating and growth-arrested *Escherichia coli* cells. *Free Radic Biol Med* 45: 708–715, 2008.

79. Maybauer DM, Maybauer MO, Szabo C, Cox RA, Westphal M, Kiss L, Horvath EM, Traber LD, Hawkins HK, Salzman AL, Southan GJ, Herndon DN, and Traber DL.

The peroxynitrite catalyst WW-85 improves pulmonary function in ovine septic shock. *Shock* 35: 148–155, 2011.

80. Maybauer DM, Maybauer MO, Szabo C, Westphal M, Traber LD, Salzman AL, Herndon DN, and Traber DL. The peroxynitrite catalyst WW-85 improves microcirculation in ovine smoke inhalation injury and septic shock. *Burns* 37: 842–850, 2011.

81. Menander-Huber KB. Orgotein in the treatment of rheumatoid arthritis. *Eur J Rheumatol Inflamm* 4: 201–211, 1981.

82. Miriyala S, Spasojevic I, Tovmasyan A, Salvemini D, Vujaskovic Z, St Clair D, and Batinic-Haberle I. Manganese superoxide dismutase, MnSOD and its mimics. *Biochim Biophys Acta* 1822: 794–814, 2012.

83. Monti DA, Mitchell E, Bazzan AJ, Littman S, Zabrecky G, Yeo CJ, Pillai MV, Newberg AB, Deshmukh S, and Levine M. Phase I evaluation of intravenous ascorbic acid in combination with gemcitabine and erlotinib in patients with metastatic pancreatic cancer. *PLoS ONE* 7: e29794, 2012.

84. Moriscot C, Candel S, Sauret V, Kerr-Conte J, Richard MJ, Favrot MC, and Benhamou PY. MnTMPyP, a metalloporphyrin-based superoxide dismutase/catalase mimetic, protects INS-1 cells and human pancreatic islets from an *in vitro* oxidative challenge. *Diabetes Metab* 33: 44–53, 2007.

85. Munroe W, Kingsley C, Durazo A, Gralla EB, Imlay JA, Srinivasan C, and Valentine JS. Only one of a wide assortment of manganese-containing SOD mimicking compounds rescues the slow aerobic growth phenotypes of both *Escherichia coli* and *Saccharomyces cerevisiae* strains lacking superoxide dismutase enzymes. *J Inorg Biochem* 101: 1875–1882, 2007.

86. Muscoli C, Cuzzocrea S, Riley DP, Zweier JL, Thiemermann C, Wang ZQ, and Salvemini D. On the selectivity of superoxide dismutase mimetics and its importance in pharmacological studies. *Br J Pharmacol* 140: 445–460, 2003.

87. Natvig DO, Imlay K, Touati D, and Hallewell RA. Human copper-zinc superoxide dismutase complements superoxide dismutase-deficient *Escherichia coli* mutants. *J Biol Chem* 262: 14697–14701, 1987.

88. Okado-Matsumoto A, Batinic-Haberle I, and Fridovich I. Complementation of SOD-deficient *Escherichia coli* by manganese porphyrin mimics of superoxide dismutase activity. *Free Radic Biol Med* 37: 401–410, 2004.

89. Pasternack RF, and Halliwell B. Superoxide dismutase activities of an iron porphyrin and other iron complexes. *J Am Chem Soc* 101: 1026–1031, 1979.

90. Peleg M, and Corradini MG. Microbial growth curves: what the models tell us and what they cannot. *Crit Rev Food Sci Nutr* 51: 917–945, 2011.

91. Pieper GM, Nilakantan V, Chen M, Zhou J, Khanna AK, Henderson JD, Jr., Johnson CP, Roza AM, and Szabo C. Protective mechanisms of a metalloporphyrinic peroxynitrite decomposition catalyst, WW85, in rat cardiac transplants. *J Pharmacol Exp Ther* 314: 53–60, 2005.

92. Rajic Z, Benov L, Kos I, Tovmasyan A, and Batinic-Haberle I. Cationic Mn porphyrins change their action from anti- to pro-oxidative in the presence of cellular reductants: relevance to understanding the beneficial therapeutic effects of SOD mimics *in vivo*. *Free Radic Biol Med* 49: S194–S194, 2010.

93. Rajic Z, Tovmasyan A, Spasojevic I, Sheng H, Lu M, Li AM, Gralla EB, Warner DS, Benov L, and Batinic-Haberle I. A new SOD mimic, Mn(III) ortho N-butoxyethylpyridylporphyrin, combines superb potency and lipophilicity with low toxicity. *Free Radic Biol Med* 52: 1828–1834, 2012.

94. Ravindranath SD, and Fridovich I. Isolation and characterization of a manganese-containing superoxide dismutase from yeast. *J Biol Chem* 250: 6107–6112, 1975.

95. Rawal M, Schroeder SR, Wagner BA, Du J, Buettner GR, and Cullen JJ. Potential of manganoporphyrins to enhance the efficacy of pharmacological ascorbate in the treatment of pancreatic cancer. *Free Radic Biol Med* 53: S115–S115, 2012.

96. Rebouças JS, DeFreitas-Silva G, Spasojevic I, Idemori YM, Benov L, and Batinic-Haberle I. Impact of electrostatics in redox modulation of oxidative stress by Mn porphyrins: protection of SOD-deficient *Escherichia coli* via alternative mechanism where Mn porphyrin acts as a Mn carrier. *Free Radic Biol Med* 45: 201–210, 2008.

97. Reboucas JS, Kos I, Vujaskovic Z, and Batinic-Haberle I. Determination of residual manganese in Mn porphyrin-based superoxide dismutase (SOD) and peroxynitrite reductase mimics. *J Pharm Biomed Anal* 50: 1088–1091, 2009.

98. Reboucas JS, Spasojevic I, and Batinic-Haberle I. Pure manganese(III) 5,10,15,20-tetrakis(4-benzoic acid)porphyrin (MnTBAP) is not a superoxide dismutase mimic in aqueous systems: a case of structure-activity relationship as a watchdog mechanism in experimental therapeutics and biology. *J Biol Inorg Chem* 13: 289–302, 2008.

99. Reboucas JS, Spasojevic I, and Batinic-Haberle I. Quality of potent Mn porphyrin-based SOD mimics and peroxynitrite scavengers for pre-clinical mechanistic/therapeutic purposes. *J Pharm Biomed Anal* 48: 1046–1049, 2008.

100. Reboucas JS, Spasojevic I, Tjahjono DH, Richaud A, Mendez F, Benov L, and Batinic-Haberle I. Redox modulation of oxidative stress by Mn porphyrin-based therapeutics: the effect of charge distribution. *Dalton Trans* 1233–1242, 2008.

101. Reddan JR, Giblin FJ, Sevilla M, Padgaonkar V, Dziedzic DC, Leverenz VR, Misra IC, Chang JS, and Pena JT. Propyl gallate is a superoxide dismutase mimic and protects cultured lens epithelial cells from H_2O_2 insult. *Exp Eye Res* 76: 49–59, 2003.

102. Riley DP, Lennon PJ, Neumann WL, and Weiss RH. Toward the rational design of superoxide dismutase mimics: mechanistic studies for the elucidation of substituent effects on the catalytic activity of macrocyclic manganese(II) complexes. *J Am Chem Soc* 119: 6522–6528, 1997.

103. Rosenthal RA, Fish B, Hill RP, Huffman KD, Lazarova Z, Mahmood J, Medhora M, Molthen R, Moulder JE, Sonis ST, Tofilon PJ, and Doctrow SR. Salen Mn complexes mitigate radiation injury in normal tissues. *Anticancer Agents Med Chem* 11: 359–372, 2011.

104. Rosenthal RA, Huffman KD, Fisette LW, Damphousse CA, Callaway WB, Malfroy B, and Doctrow SR. Orally available Mn porphyrins with superoxide dismutase and catalase activities. *J Biol Inorg Chem* 14: 979–991, 2009.

105. Sambrook J, Fritsch EF, and Maniatis T. *Molecular Cloning*. New York: Cold Spring Harbor Laboratory Press, 1989.

106. Sanchez RJ, Srinivasan C, Munroe WH, Wallace MA, Martins J, Kao TY, Le K, Gralla EB, and Valentine JS. Exogenous manganous ion at millimolar levels rescues all known dioxygen-sensitive phenotypes of yeast lacking CuZnSOD. *J Biol Inorg Chem* 10: 913–923, 2005.

107. Schreier S, Malheiros SVP, and De Paula E. Surface active drugs: self-association and interaction with membranes and surfactants. Physicochemical and biological aspects. *Biochim Biophys Acta* 1508: 210–234, 2000.

108. Sheng H, Chaparro RE, Sasaki T, Izutsu M, Pearlstein RD, Tovmasyan A, and Warner DS. Metalloporphyrins as

therapeutic catalytic oxidoreductants in central nervous system disorders. *Antioxid Redox Signal* 20: 2437–2464, 2014.

109. Shuaib A, Lees KR, Lyden P, Grotta J, Davalos A, Davis SM, Diener HC, Ashwood T, Wasiewski WW, and Emeribe U. NXY-059 for the treatment of acute ischemic stroke. *N Engl J Med* 357: 562–571, 2007.

110. Soule BP, Hyodo F, Matsumoto K, Simone NL, Cook JA, Krishna MC, and Mitchell JB. The chemistry and biology of nitroxide compounds. *Free Radic Biol Med* 42: 1632–1650, 2007.

111. Spasojevic I, Kos I, Benov LT, Rajic Z, Fels D, Dedeugd C, Ye X, Vujaskovic Z, Reboucas JS, Leong KW, Dewhirst MW, and Batinic-Haberle I. Bioavailability of metalloporphyrin-based SOD mimics is greatly influenced by a single charge residing on a Mn site. *Free Radic Res* 45: 188–200, 2011.

112. Spasojevic I, Li A, Tovmasyan A, Rajic Z, Salvemini D, St Clair D, Valentine JS, Vujaskovic Z, Gralla EB, and Batinic-Haberle I. Accumulation of porphyrin-based SOD mimics in mitochondria is proportional to their lipophilicity: *S-cerevisiae* study of ortho Mn(III) N-alkylpyridylporphyrins. *Free Radic Biol Med* 49: S199–S199, 2010.

113. Stojiljkovic I, Evavold BD, and Kumar V. Antimicrobial properties of porphyrins. *Expert Opin Investig Drugs* 10: 309–320, 2001.

114. Strain J, Lorenz CR, Bode J, Garland S, Smolen GA, Ta DT, Vickery LE, and Culotta VC. Suppressors of superoxide dismutase (SOD1) deficiency in *Saccharomyces cerevisiae*: identification of proteins predicted to mediate iron-sulfur cluster assembly. *J Biol Chem* 273: 31138–31144, 1998.

115. Szabo C, Mabley JG, Moeller SM, Shimanovich R, Pacher P, Virag L, Soriano FG, Van Duzer JH, Williams W, Salzman AL, and Groves JT. Part I: pathogenetic role of peroxynitrite in the development of diabetes and diabetic vascular complications: studies with FP15, a novel potent peroxynitrite decomposition catalyst. *Mol Med* 8: 571–580, 2002.

116. Szabo G, Loganathan S, Merkely B, Groves JT, Karck M, Szabo C, and Radovits T. Catalytic peroxynitrite decomposition improves reperfusion injury after heart transplantation. *J Thorac Cardiovasc Surg* 143: 1443–1449, 2012.

117. Tian J, Peehl DM, and Knox SJ. Metalloporphyrin synergizes with ascorbic acid to inhibit cancer cell growth through Fenton chemistry. *Cancer Biother Radiopharm* 25: 439–448, 2010.

118. Touati D. Molecular genetics of superoxide dismutases. *Free Radic Biol Med* 5: 393–402, 1988.

119. Touati D. The molecular genetics of superoxide dismutase in *E. coli*. *Free Radic Res Commun* 12–13 Pt 1: 379–382, 1991.

120. Tovmasyan A, Sheng H, Weitner T, Arulpragasam A, Lu M, Warner DS, Vujaskovic Z, Spasojevic I, and Batinic-Haberle I. Design, mechanism of action, bioavailability and therapeutic effects of Mn porphyrin-based redox modulators. *Med Princ Pract* 22: 103–130, 2013.

121. Tovmasyan A, Weitner T, Roberts E, Jaramillo M, Spasojevic I, Leong KW, Tome M, Benov L, and Batinic-Haberle I. Understanding differences in mechanisms of action of Fe vs. Mn porphyrins: comparison of their reactivities towards cellular reductants and reactive species. *Free Radic Biol Med* 53: S120, 2012.

122. Tovmasyan A, Weitner T, Sheng H, Lu M, Rajic Z, Warner DS, Spasojevic I, Reboucas JS, Benov L, and Batinic-Haberle I. Differential coordination demands in Fe versus Mn water-soluble cationic metalloporphyrins translate into remarkably different aqueous redox chemistry and biology. *Inorg Chem* 52: 5677–5691, 2013.

123. Tovmasyan AG, Rajic Z, Spasojevic I, Reboucas JS, Chen X, Salvemini D, Sheng H, Warner DS, Benov L, and Batinic-Haberle I. Methoxy-derivatization of alkyl chains increases the *in vivo* efficacy of cationic Mn porphyrins: synthesis, characterization, SOD-like activity, and SOD-deficient *E. coli* study of meta Mn(iii) N-methoxyalkylpyridylporphyrins. *Dalton Trans* 40: 4111–4121, 2011.

124. Van Loon APGM, Pesold-Hurt B, and Schatz G. A yeast mutant lacking mitochondrial manganese-superoxide dismutase is hypersensitive to oxygen. *Proc Natl Acad Sci U S A* 83: 3820–3824, 1986.

125. Wallace MA, Liou LL, Martins J, Clement MHS, Bailey S, Longo VD, Valentine JS, and Gralla EB. Superoxide inhibits 4Fe-4S cluster enzymes involved in amino acid biosynthesis: cross-compartment protection by CuZn-superoxide dismutase. *J Biol Chem* 279: 32055–32062, 2004.

126. Weitner T, Kos I, Sheng H, Tovmasyan A, Reboucas JS, Fan P, Warner DS, Vujaskovic Z, Batinic-Haberle I, and Spasojevic I. Comprehensive pharmacokinetic studies and oral bioavailability of two Mn porphyrin-based SOD mimics, MnTE-2-PyP(5+) and MnTnHex-2-PyP(5+). *Free Radic Biol Med* 58: 73–80, 2013.

127. Welsh JL, Wagner BA, Van'T Erve TJ, Zehr PS, Berg DJ, Halfdanarson TR, Yee NS, Bodeker KL, Du J, Roberts Ii LJ, Drisko J, Levine M, Buettner GR, and Cullen JJ. Pharmacological ascorbate with gemcitabine for the control of metastatic and node-positive pancreatic cancer (PAC-MAN): results from a phase I clinical trial. *Cancer Chemother Pharmacol* 71: 765–775, 2013.

128. Wu L, Shan Y, and Liu D. Stability, disposition, and penetration of catalytic antioxidants Mn-porphyrin and Mn-salen and of methylprednisolone in spinal cord injury. *Cent Nerv Syst Agents Med Chem* 12: 122–130, 2012.

129. Xiu Fen L, Elashvili I, Gralla EB, Valentine JS, Lapinskas P, and Culotta VC. Yeast lacking superoxide dismutase: isolation of genetic suppressors. *J Biol Chem* 267: 18298–18302, 1992.

130. Ye X, Fels D, Tovmasyan A, Aird KM, Dedeugd C, Allensworth JL, Kos I, Park W, Spasojevic I, Devi GR, Dewhirst MW, Leong KW, and Batinic-Haberle I. Cytotoxic effects of Mn(III) N-alkylpyridylporphyrins in the presence of cellular reductant, ascorbate. *Free Radic Res* 45: 1289–1306, 2011.

131. Zyracka E, Zadrag R, Kozioł S, Krzepiłko A, Bartosz G, and Biliński T. Yeast as a biosensor for antioxidants: simple growth tests employing a *Saccharomyces cerevisiae* mutant defective in superoxide dismutase. *Acta Biochim Pol* 52: 679–684, 2005.

Address correspondence to:
Dr. Ludmil Benov
Department of Biochemistry
Faculty of Medicine
Kuwait University
P. O. Box 24923 Safat
1310 Kuwait

E-mail: lbenov@hsc.edu.kw

Abbreviations Used

5AA = five amino acid, minimal, restricted medium

$E_{1/2}$ = half-wave reduction potential

EG118 and EG103 = SOD-deficient and SOD-proficient *Saccharomyces cerevisiae* strains, respectively

EUK-134 and EUK-8 = Mn salen derivatives

FeP = Fe porphyrin

FeTM-2-PyP^{5+} = Fe(III) *meso*-tetrakis(*N*-methylpyridinium-2-yl)porphyrin

FeTM-3-PyP^{5+} = Fe(III) *meso*-tetrakis(*N*-methylpyridinium-3-yl)porphyrin

FeTM-4-PyP^{5+} = Fe(III) *meso*-tetrakis(*N*-methylpyridinium-4-yl)porphyrin

FeTE-2-PyP^{5+} = Fe(III) *meso*-tetrakis(*N*-ethylpyridinium-2-yl)porphyrin

FP-15 = Fe (III) *meso*-tetrakis(*N*-(1-(2-(2(-2-methoxyethoxy)ethoxy)ethyl)pyridinium-2-yl) porphyrin

H_2O_2 = hydrogen peroxide

INO-4885 = Fe(III) *meso*-tetrakis[*N*-(4-carboxylatobenzyl)pyridinium-2-yl]porphyrin

JI132 and AB1157 = SOD-deficient and SOD-proficient *Escherichia coli* strains, respectively

M40403 = cyclic polyamine

M9CA = casamino acid complete medium

Mn(III) *meso*-tetrakis(*N*-alkylpyridinium-2-yl)porphyrins, alkyl being methyl (M, MnTM-2-PyP^{5++}, AEOL10112), ethyl (E, MnTE-2-PyP^{5++}, AEOL10113, BMX-010), n-propyl (nPr, MnTnPr-2-PyP^{5+}), n-butyl (nBu, MnTnBu-2-PyP^{5+}), n-hexyl (nHex, MnTnHex-2-PyP^{5+}), n-heptyl (nHep, MnTnHep-2-PyP^{5+}), n-octyl (nOct, MnTnOct-2-PyP^{5+})

Mn(III) *meso*-tetrakis(*N*-alkylpyridinium-3-yl)porphyrins, alkyl being methyl (M, MnTM-3-PyP^{5+}), ethyl (E, MnTE-3-PyP^{5+}), n-propyl (nPr, MnTnPr-3-PyP^{5+}), n-butyl (nBu, MnTnBu-3-PyP^{5+}), n-hexyl (nHex, MnTnHex-3-PyP^{5+})

MnBr$_8$TBAP^{3-} = Mn(III) *β*-octabromo-*meso*-tetrakis(4-carboxylatophenyl)porphyrin, also known as

MnBr$_8$TM-3(or 4)-PyP^{4+} = Mn(III) *β*-octabromo-*meso*-tetrakis(*N*-methylpyridinium-3(or 4)-yl))porphyrin

MnBr$_8$TSPP^{3-} = Mn(III) *β*-octabromo-*meso*-tetrakis(4-sulfonatophenyl)porphyrin

MnP = Mn porphyrin (charges of MnPs are omitted in figures but not in figure legends)

MnT(2,6-Cl$_2$-3-SO$_3$-P)P^{3-} = Mn(III) *meso*-tetrakis(2,6-dichloro-3-sulfonatophenyl)porphyrin

MnT(TFTeMa)P^{5+} = Mn(III) *meso*-tetrakis(2,3,5,6 tetrafluoro-*N,N,N*-trimethylanilinium-4-yl)porphyrin

MnT(TrMA)P^{5+} = Mn(III) meso-tetrakis(2,3,5,6 tetrafluoro- *N,N,N*-trimethylanilinium-4-yl)porphyrin

MnTBAP^{3-} = Mn(III) *meso*-tetrakis(4-carboxyphenyl)porphyrin, also known as MnTCPP^{3-} and AEOL10201

MnTDE-2-ImP^{5+} = Mn(III) *meso*-tetrakis(*N,N'*-diethylimidazolium-2-yl)porphyrin, AEOL10150

MnTDMOE-2-ImP^{5+} = Mn(III) *meso*-tetrakis[*N,N'*-di(2-methoxyethyl)imidazolium-2-yl]porphyrin

MnTM-4-PyP^{5+} = Mn(III) *meso*-tetrakis(*N*-methylpyridinium-4-yl)porphyrin

MnTM,MOE-2-ImP^{5+} = Mn(III) *meso*-tetrakis[(*N*-methyl-*N'*-methoxethyl)imidazolium-2-yl]porphyrin

MnTMOE-3-PyP^{5+} = Mn(III) *meso*-tetrakis(*N*-(2'-methoxyethyl)pyridinium-3-yl)porphyrin

MnTMOHex-3-PyP^{5+} = Mn(III) *meso*-tetrakis(*N*-(6'-methoxyhexyl)pyridinium-3-yl)porphyrin

MnTnBuOE-2-PyP^{5+} = Mn(III) *meso*-tetrakis(*N*-(n-butoxyethyl)pyridinium-2-yl)porphyrin, also BMX-001

MnTSPP^{3-} = Mn(III) *meso*-tetrakis(4-sulfonatophenyl)porphyrin

NaCl = sodium chloride

NH$_4$PF$_6$ = ammonium hexafluorophosphate

NHE = normal hydrogen electrode

NIH = National Institutes of Health

nitrone = NXY-059, disulfonated PBN, phenyl-t*ert*-butylnitrone

$O_2^{\bullet-}$ = superoxide

ONOO$^-$ = peroxynitrite

ROS = reactive oxygen species

SE = standard error

SOD = superoxide dismutase

TBACl = tetra-n-butylammonium chloride

tempol = 4-OH-2,2,6,6,-tetramethylpiperidine-1-oxyl

WW-85 = Fe(III) *meso*-tetrakis(*N*-carboxylatobenzylpyridyl)porphyrin